Soria-Verdugo, Antonio; Goos, Elke; García-Hernando, Nestor; Riedel, Uwe. (2018). Analyzing the pyrolysis kinetics of several microalgae species by various differential and integral isoconversional kinetic methods and the Distributed Activation Energy Model, *Algal Research*, v. 32, pp.: 11-29.

DOI: https://doi.org/10.1016/j.algal.2018.03.005

Analyzing the pyrolysis kinetics of several microalgae species by various differential and integral isoconversional kinetic methods and the Distributed Activation Energy Model

Antonio Soria-Verdugo[a]*, Elke Goos[b], Nestor García-Hernando[a], Uwe Riedel[b]

[a] *Carlos III University of Madrid (Spain), Energy Systems Engineering Group, Thermal and Fluids Engineering Department. Avda. de la Universidad 30, 28911 Leganés (Madrid, Spain).*

[b] *Deutsches Zentrum für Luft- und Raumfahrt e.V. (DLR, German Aerospace Center), Institute of Combustion Technology, Pfaffenwaldring 38-40, 70569 Stuttgart (Germany).*

** corresponding author: asoria@ing.uc3m.es Tel.: +34916248465.*

Abstract

The pyrolysis kinetics of the microalgae *Chlorella Vulgaris* (CV), *Isochrysis Galbana* (IG), *Nannochloropsis Gaditana* (NG), *Nannochloropsis Limnetica* (NL), *Phaeodactylum Tricornutum* (PT), and *Spirulina Platensis* (SP) were studied by non-isothermal thermogravimetric analysis conducted at nine different constant heating rates. The kinetic parameters of each microalgae species were calculated using several kinetic methods, such as those of Kissinger, Friedman, Ozawa-Flynn-Wall (OFW), Kissinger-Akahira-Sunose (KAS), Vyazovkin, and the simplified Distributed Activation Energy Model (DAEM). The results show that the kinetic parameters calculated from the integral isoconversional methods OFW, KAS and Vyazovkin are similar to those determined by applying the simplified DAEM. In contrast, application of the differential isoconversional method of

Friedman led to moderate deviations in the activation energies and pre-exponential factors computed, whereas the unique values of the kinetic parameters determined by the Kissinger method resulted in the highest deviations.

***Keywords*:** Microalgae, Pyrolysis kinetics, Thermogravimetric Analysis (TGA), Isoconversional methods.

Nomenclature:

A	Pre-exponential factor [s^{-1}].
α	Conversion [%].
β	Heating rate [K s^{-1}].
E	Activation energy [J mol^{-1}].
g	Stoichiometric coefficient within a reaction for a gaseous product [-].
$G_{(g)}$	Gaseous product [-].
k	Rate coefficient of a first order reaction [s^{-1}].
m	Mass of the sample remaining at time t [kg].
m_0	Initial mass of the sample [kg].
m_f	Final mass of the sample [kg].
n	Order of the pyrolysis reactions [-].
N	Number of TGA curves obtained at different heating rates [-].
R	Universal gas constant [J mol^{-1} K^{-1}].
s_1	Stoichiometric coefficient within a reaction for a solid reactant [-].
s_2	Stoichiometric coefficient within a reaction for a solid product [-].
$S1_{(s)}$	Solid reactant
$S2_{(s)}$	Solid product

t Time [s].

T Temperature [K].

T_0 Ambient temperature [K].

T_{max} Temperature at maximum rate of reaction [K].

Abbreviations:

CV *Chlorella Vulgaris*.

DAEM Distributed Activation Energy Model.

DTG Derivative Thermogravimetric.

FAME Fatty Acid Methyl Ester.

HHV High Heating Value.

IG *Isochrysis Galbana*.

KAS Kissinger-Akahira-Sunose.

NG *Nannochloropsis Gaditana*.

NL *Nannochloropsis Limnetica*.

OFW Ozawa-Flynn-Wall.

PT *Phaeodactylum Tricornutum*.

SP *Spirulina Platensis*.

TGA Thermogravimetric Analysis.

1. Introduction

Pyrolysis of microalgae produces solid, liquid, and gaseous products of interest, which can be employed as sources of energy and/or chemicals. Pyrolysis is a process by which the biomass is thermally degraded in the absence of oxygen at moderate temperatures between 350 ºC and 700 ºC [1]. Knowledge of the thermal behavior of microalgae during the pyrolysis process, especially their

apparent kinetics, is a crucial factor for the efficient use of this type of biomass as a source to produce biofuels [2]. A deeper knowledge of the pyrolysis process will serve as a useful tool for the design and operation of pyrolysis reactors with higher efficiency [3]. A widely used technique employed to study the pyrolysis of solid fuels is thermogravimetric analysis (TGA), which permits the calculation of pyrolysis kinetic parameters from the measurement of the evolution of the mass of a sample subjected to a temperature increase in an inert atmosphere. Based on TGA measurements, several mathematical models have been developed to describe the kinetic mechanism of the pyrolysis process, such as the Kissinger method [4, 5], the single step model [6], the parallel reactions model [7], the three pseudo-components model [8], the sectional approach model [9], the Distributed Activation Energy Model (DAEM) [10], or isoconversional methods [11]. Isoconversional methods can be further divided into two categories [12]: differential methods and integral methods. The most common differential method is the Friedman method [13], whereas there is a wide variety of integral methods, among which the most commonly used are the Ozawa-Flynn-Wall (OFW) method [14, 15], the Kissinger-Akahira-Sunose (KAS) method [4, 16], and the Vyazovkin method [17]. Integral methods are more universal due to their higher tolerance to experimental noise compared to differential methods, for which the use of derivatives propagates the effect of noise, reducing the accuracy of the results [18].

The kinetics of microalgae pyrolysis based on TGA measurements was recently reviewed by Bach and Chen [19]. The kinetics of multiple microalgae species has been studied applying either kinetic fitting or kinetic free models. For kinetic fitting models, the single reaction model, which assumes that microalgae are directly

decomposed into char and volatiles, is very simple, but the fitting quality of this model to describe the pyrolysis of microalgae samples is quite poor [19]. Among the kinetic fitting models, multiple parallel reaction models are widely used to describe microalgae pyrolysis. These models were originally developed to characterize the pyrolysis of the three main components of lignocellulosic biomass, i.e., hemicellulose, cellulose and lignin [20]. Due to differences in composition between lignocellulosic and microalgal biomass, the number of parallel reactions for the model was modified to account for the pyrolysis of carbohydrates, proteins, lipids, and other minor components of microalgae [21, 22].

In contrast to fitting kinetic models, free kinetic models require no assumptions about the form of the conversion rate pyrolysis curve. Using kinetic free models to describe the pyrolysis of microalgae, the Vyazovkin method was applied by Gai et al. [23] to analyze the pyrolysis of *Chlorella Pyrenoidosa* and *Spirulina Platensis*, whereas the Kissinger method was employed to study the pyrolysis of periphytic microalgae [24] and the salt-water cord grass *Spartina Alterniflora* [25]. The differential isoconversional method of Friedman was applied to describe the pyrolysis of the red algae *Kappaphycus Alvarezii* [26], and the salt-water cord grass *Spartina Alterniflora* [25]. The integral isoconversional methods of OFW and KAS have been applied to determine the pyrolysis kinetics of a broad range of microalgae species, including *Chlorella sp.* [27], *Chlorella Vulgaris* [28, 29, 30, 31, 32], *Dunaliella Tertiolecta* [33], *Kappaphycus Alvarezii* [26], *Tetraselmis Suecica* [27], and the salt-water cord grass *Spartina Alterniflora* [27]. The simplified Distributed Activation Energy Model (DAEM) has also been widely applied to investigate the pyrolysis of several microalgae species, for instance

Chlorella Humicola [34], *Chlorella Pyrenoidosa* [35], *Chlorella Sorokiniana* [36], *Chlorella Vulgaris* [37], *Dunaliella Tertiolecta* [38], *Monoraphidium* [36], *Nannochloropsis Oculata* [2], and *Tetraselmis sp.* [2]. Although many studies concerning the kinetics of microalgae pyrolysis are based on TGA measurements, they are limited in number compared to studies in other reactors such as fixed or fluidized beds [19]. Furthermore, most studies on the pyrolysis kinetics of microalgae available in the literature are based on a reduced number of TGA curves and, due to the limited number of investigation points on which they are based, these kinetic models cannot provide information about the fit quality of the models [19].

In this work, the pyrolysis kinetics of several microalgae species was investigated using non-isothermal thermogravimetric analysis (TGA). Six microalgae species were selected for the pyrolysis study to cover a broad range of biological and chemical properties, as well as growing conditions: *Chlorella Vulgaris* (CV), *Isochrysis Galbana* (IG), *Nannochloropsis Gaditana* (NG), *Nannochloropsis Limnetica* (NL), *Phaeodactylum Tricornutum* (PT), and *Spirulina Platensis* (SP). In contrast to studies available in the literature that are typically based on a reduced number of TGA curves, the TGA pyrolysis measurements were conducted for each microalgae species, using nine different constant heating rates of 10, 13, 16, 19, 22, 25, 30, 35, and 40 K/min over a temperature range from 100 ºC to 800 ºC. The experimental results obtained from the TGA pyrolysis measurements were employed to calculate the pyrolysis kinetics parameters of the samples applying various kinetic methods: Kissinger, Friedman, OFW, KAS, Vyazovkin, and simplified DAEM. Moreover, the high number of TGA curves employed to analyze the pyrolysis kinetics of each microalgae sample permits

characterization of the experimental measurements reliability and the fit capability of the kinetic models based on the quality of the linearization of the Arrhenius plots [39].

2. Pyrolysis kinetics

The kinetics of chemical reactions in solids, such as $s_1S1_{(s)} \rightarrow s_2S2_{(s)} + gG_{(g)}$, can be described by the rate of disappearance of the reactant *S1* [6], which is usually determined as a derivation of the law of mass action, originally proposed by Guldberg and Waage [40]:

$$\frac{d\alpha}{dt} = k(T)\, f(\alpha), \tag{1}$$

where α is the conversion, t is the time, $d\alpha/dt$ is the rate of reaction, $k(T)$ is the rate coefficient at an absolute temperature T, and $f(\alpha)$ is a function of α, with its exact form depending on the order of the kinetic model. The conversion α of the sample can be calculated from the mass loss of the sample during the chemical reaction:

$$\alpha = 1 - \frac{m - m_f}{m_0 - m_f} = \frac{m_0 - m}{m_0 - m_f}, \tag{2}$$

where m is the mass of the sample remaining at time t, m_f is the final mass of the sample when the reaction is completed, and m_0 is the initial mass of the sample.

The reaction rate coefficient $k(T)$ can be expressed as a function of the absolute temperature T using various equations [41], however, the most widely used expression for the rate coefficient is [42]:

$$k(T) = A\exp\left(-\frac{E}{RT}\right), \tag{3}$$

where A is the pre-exponential factor, E is the activation energy, and R is the universal gas constant.

Considering the Arrhenius relation for the rate coefficient and the absolute temperature, the rate of reaction, Eq. (1), can be written in differential form as:

$$\frac{d\alpha}{dt} = A\exp\left(-\frac{E}{RT}\right) f(\alpha). \tag{4}$$

For non-isothermal conditions, when the absolute temperature increases with time at a constant heating rate, $\beta = dT/dt$, Eq. (4) can be represented as:

$$\frac{d\alpha}{dT} = \frac{A}{\beta}\exp\left(-\frac{E}{RT}\right) f(\alpha), \tag{5}$$

which, assuming the pre-exponential factor A to be independent of the temperature, can be integrated to obtain the integral form of the rate equation:

$$g(\alpha) = \int_0^{\alpha} \frac{d\alpha}{f(\alpha)} = \frac{A}{\beta}\int_{T_0}^{T} \exp\left(-\frac{E}{RT}\right) dT \approx \frac{A}{\beta}\int_0^{T} \exp\left(-\frac{E}{RT}\right) dT, \tag{6}$$

where the lower integration limit in the last integral can be approximated to 0 since the rate of reaction is negligibly low for temperatures below ambient temperature T_0 [14].

The kinetic parameters of solid chemical reactions can be obtained using isoconversional methods or model-fitting methods. In contrast to model-fitting methods, where an assumption of the form of $f(\alpha)$ is required, isoconversional methods permit direct determination of the kinetic parameters from the

thermogravimetric data of the sample. Therefore, the kinetic parameters calculated via isoconversional methods are more reliable and consistent [43]. Isoconversional methods can be applied to multistep reactions, such as those occurring during the pyrolysis of solid fuels [17]. They are based on the isoconversional principle, whose main assumption is temperature independency of the activation energy and the pre-exponential factor. However, both parameters are still interrelated functions of the conversion α [13, 14, 15].

According to the basic equation employed, isoconversional methods can be further divided into two categories [12]: differential methods, such as the Friedman method [13], which work directly with the differential form of the rate equation, Eq. (4); and integral methods, such as the Ozawa-Flynn-Wall (OFW) method [14, 15], the Kissinger-Akahira-Sunose (KAS) method [4, 16], and the Vyazovkin method [17], which use the integral form of the rate equation, Eq. (6).

The Arrhenius equation for the differential isoconversional method of Friedman, considering a first-order reaction, is [13]:

$$Ln\left(\frac{d\alpha}{dt}\right) = Ln\left(A\left(1-\alpha\right)\right) - \frac{E}{RT}. \tag{7}$$

The Ozawa-Flynn-Wall method is based on Doyle's approximation [44], resulting in the following Arrhenius equation [14, 15]:

$$Ln\left(\beta\right) = Ln\left(\frac{AE}{Rg\left(\alpha\right)}\right) - 5.3305 - 1.052\frac{E}{RT}. \tag{8}$$

The Kissinger-Akahira-Sunose method [4, 16] improved the accuracy of the OFW method, using the approximation of Coats-Redfern [6]. The Arrhenius equation for KAS reads as follows:

$$Ln\left(\frac{\beta}{T^2}\right) = Ln\left(\frac{AR}{Eg(\alpha)}\right) - \frac{E}{RT}, \tag{9}$$

Even though the Vyazovkin method is also an integral isoconversional method, it is based on minimization of the function shown in Eq. (10) [17] instead of an Arrhenius equation. To minimize this function, the Vyazovkin method uses the approximation of Senum-Yang [45].

$$\left| N(N-1) - \sum_{i=1}^{N}\sum_{j=1}^{N} \frac{I\left(E_\alpha, T_{\alpha,i}\right)/\beta_i}{I\left(E_\alpha, T_{\alpha,j}\right)/\beta_j} \right| = \min \qquad (\text{with } i \neq j). \tag{10}$$

The simplified Distributed Activation Energy Model (DAEM) assumes first-order reactions and is also based on the approximation of Coats-Redfern [6]. The Arrhenius equation obtained for the simplified DAEM is [46, 47]:

$$Ln\left(\frac{\beta}{T^2}\right) = Ln\left(\frac{AR}{E}\right) + 0.6075 - \frac{E}{RT}. \tag{11}$$

This Arrhenius equation is valid exclusively for linear heating rates of solid fuels, i.e., for a constant value of β. However, the Arrhenius equations obtained by applying the simplified DAEM for parabolic and exponential temperature profiles can be found in Soria-Verdugo et al. [48].

In contrast to OFW, KAS, Vyazovkin and simplified DAEM, the Kissinger method is based on the differential form of the rate equation, Eq. (4), yielding for the first-order reaction the following Arrhenius equation [4]:

$$Ln\left(\frac{\beta}{T_{max}^2}\right) = Ln\left(\frac{AR}{E}\right) - \frac{E}{RT_{max}}. \quad (12)$$

A detailed description of the mathematical derivation of these kinetic models can be found in Appendix 1.

3. Materials and methods

3.1. Microalgae characterization

The microalgae investigated in this study are, in alphabetical order, *Chlorella Vulgaris*, *Isochrysis Galbana*, *Nannochloropsis Gaditana*, *Nannochloropsis Limnetica*, *Phaeodactylum Tricornutum,* and *Spirulina Platensis*. The microalgae samples investigated in this study were cultivated and predried by AlgaEnergy S.A., (Alcobendas, Madrid, Spain) in 2016 (CV) and 2017 (IG, NG, NL. PT, SP). The CV sample cultivated in 2016 was the focus of a previous pyrolysis study [37].

3.1.1 *Chlorella Vulgaris*

Chlorella Vulgaris are green algae first described in 1890 by Beyerinck [49], who a year earlier found the algae in a small pond near Delft (Netherlands). Since then, these microalgae have been broadly investigated for more than 100 years.

The Chlorophyta *Chlorella Vulgaris* belong to the class Trebouxiophyceae, according to the systematic classification of plants, called taxonomy. These mono-cellular green microalgae have a spherical shape with a diameter of 3 – 10 μm and grow in flowing or standing fresh and brackish water at moderate temperatures, e.g., in Europe, as well as at polar and tropical water temperatures [50]. The dried algae samples contain approximately 50% protein, minerals as

calcium, magnesium, potassium, iron, zinc, manganese, and sulfur and approximately 5% (dry ash free weight) various unsaturated fatty acids, which include essential fatty acids for animals and humans, such as alpha-linolenic acid and carotenoids. Therefore, these microalgae are used as a healthful food, food supplement, and feed surrogates for animals, e.g., fish or chicken. For application as a source for biodiesel generation, compared to other microalgae species such as *Nannochloropis sp.*, the oil content of *Chlorella Vulgaris* is too low for economic biodiesel production [51].

3.1.2. *Isochrysis Galbana*

Isochrysis Galbana is a gold-brown marine microalga belonging to the division of Haptophyta in the class Haptophyceae. It was first isolated in 1938 in Port Erin, where it grows in seawater in a fish pond at the Marine Biological Station on the Isle of Man (United Kingdom) [52].

The motile cells of *Isochrysis Galbana* are usually somewhat ellipsoidal, with lengths of 5 – 6 μm, widths of 2 – 4 μm, and thicknesses of 2.5 – 3 μm. However, they can change shape, resulting in considerable variation between individuals. They have two equal flagella with a length varying from once to twice the cell length and grow well in open ponds. These microalgae contain approximately 24% carbohydrates, approximately 18% monounsaturated C16-alkenoic acid, and a distribution of polyunsaturated fatty acids (PUFA), including approximately 24% eicosapentaenoic acid (EPA), up to 10% docosahexaenoic acid (DHA), and approximately 4% arachidonic acid (ARA). These contents are of great interest for the cosmetics industry. Additionally, these marine microalgae also contain

between 6% and 8% minerals, are ideally suitable for feeding all types of mollusks, and can be used in general for animal nutrition [53].

3.1.3. *Nannochloropsis sp*.

Nannochloropsis is a genus of algae comprising six known species, namely, *N. Gaditana*, *N. Granulate*, *N. Limnetica*, *N. Oceanica*, *N. Oculata*, and *N. Salina.* Of these, in this study the pyrolysis behavior of *N. Gaditana* and *N. Limnetica* were investigated.

Nannochloropsis Gaditana, a marine species of Eustigmatophyceae, was first described in terms of morphology, ultrastructure, its pigments composition, and growth physiology by Lubián [54], who isolated it from Cádiz Bay (Spain). These microalgae are elliptical species with dimensions of 3.5 – 4 and 2.5 – 3 μm, and no other distinct morphological features. Therefore, distinction from other *Nannochlorpsis* species using only light or electron microscopy techniques is nearly impossible. Their characterization by gene and DNR sequence analysis is therefore recommended [55].

Nannochloropsis Limnetica was the first characterized fresh water species of *Nannochloropsis,* found in a highly productive village pond in Schwarz, Sachsen-Anhalt (Germany) [56]. These microalgae also grow in fresh water at moderate temperatures in other lakes in Germany, North America, and Russia [57, 58].

The marine microalgae *Nannochloropsis* has proved suitable as a raw material for biofuel production [51]. They have a high oil content of approximately 29% of dry weight, which can be increased to approximately 50% by growing the microalgae under nitrogen shortage. Methanol-esterified oil produced from

Nannochloropsis sp. satisfies the European Standard [59], which specifies a limit of 12 wt% and 1 wt%, respectively, for linolenic (C18:3) and polyunsaturated ester (≥ 4 double bonds) resulting from the esterification of the unsaturated fatty acids of the microalgae oil for use of FAME as biodiesel. In addition, the reactivity of the fuel to oxidation and rancidification is limited by the European Standard [59] for FAME use in diesel engines to a maximum iodine value of <120 g I_2 per 100 g of fuel to ensure the long-term stability of automotive fuels. The microalgae oil extracted from *Nannochloropsis sp.* has an iodine value of 52 g I_2 per 100 g oil [51], as determined by European Standard method [60], satisfying the aforementioned European biodiesel specification, in contrast to some vegetable bio-oils obtained, e.g., from soybeans or sunflowers, which have iodine values higher than 120 g I_2 per 100 g oil, requiring further treatment such as hydrogenation prior to their use as biodiesel.

3.1.4. *Phaeodactylum Tricornutum*

Phaeodactylum Tricornutum is a cosmopolitan marine Bacillariophyceae or diatom, a unicellular brown alga, which has been known for hundreds of years [61]. These microalgae are easily recognized by their cell coverings, consisting of two silica dishes, which result in a high ash content in their chemical analysis. They grow in brackish and in marine waters and, for industrial production, in open ponds and basins. This genus of microalgae can vary their buoyancy by adjusting the oil content in their cells to optimize the incidence of light on their surface.

The high concentration on eicosapentaenoic acid (EPA) of *Phaeodactylum Tricornutum* is particularly interesting for nutrition production [62]. In addition to oil content, which can reach up to 60% of dry weight especially under nitrogen-

starvation, their main food reserve is chrysolaminarin, a small glucose polymer. Due to their high productivity and accumulation of oils, *Phaeodactylum Tricornutum* may represent a future source for production of both unusual fatty acids and fuel, especially biodiesel produced by esterification.

3.1.5. *Spirulina Platensis / Arthrospira Platensis*

This microalga is a Cyanobacterium that grows with broad morphological variability as a blue-green alga. Its morphology, ultrastructure and taxonomy were described by Tomasselli [63]. This species was accidently merged by Geitler [64] with the genus *Spirulina* rather than the genus *Arthrospira.* The different taxonomic position of *Spirulina* species and *Arthrospira spp*. among Cyanobacteria was justified later by Nelissen et al. [65], according to genetic analysis of the phylogenetic relationships. Although it is now generally accepted that two separate genera *Arthrospira* and *Spirulina* exist, taxonomical confusion and discussion on this topic continues. For tradition's sake, the wrong name *Spirulina* is used today in nearly all applications such as food supply [66], healthy food additives [67], or technical applications such as biomass conversion processes.

These algae grow naturally mainly in tropical and subtropical regions in brackish and fresh warm waters with high carbonate, bicarbonate and/or salt concentrations, as well as under high pH, such as a natron lake in Chad and a saline marsh in USA [68]. Approximately 2/3 of their biomass dry weight consists of proteins [66], while the total carbohydrate content is between 10% and 20% and the total lipid content is approximately 10%, with high amounts of polyunsaturated fatty acids (PUFAs), including essential ω-6 fatty acid and γ-

linolenic acid (GLA) [69]. Further components of these microalgae are minerals, vitamins, such as carotenoids, and photosynthetic pigments, e.g., chlorophyll. The biomass composition of *Spirulina Platensis* is affected by the growth conditions, which are normally considered in their industrial production.

3.2. Proximate and ultimate analyses of microalgae

A basic characterization of all microalgae species was performed, consisting of a proximate analysis, an ultimate analysis, and a heating value test. The proximate analysis was conducted in the TGA Q500 as described in section 3. The volatile matter content was determined as the percentage of mass released by a dry sample subjected to a heating process up to 900 ºC in an inert atmosphere, while the ash content was measured as the percentage of mass remaining after heating to 550 ºC in an oxidant atmosphere.

The ultimate analysis of the various microalgae species was performed in a LECO TruSpec CHN Macro and TruSpec S analyser. The carbon, hydrogen, and sulphur contents of the samples were measured by infrared absorption of the exhaust gases via complete combustion of the samples in pure oxygen, whereas a thermal conductivity cell was employed to determine the nitrogen content. The equipment has a precision of ±0.5% for carbon and nitrogen contents and ±1% for hydrogen and sulphur contents.

The High Heating Value (HHV) of the samples was measured in an isoperibolic calorimeter Parr 6300 with a precision of 0.1% and a linearity of 0.05% across the operating range. The equipment has a temperature resolution of 0.0001 ºC. The results of the basic characterization of the six microalgae species studied are shown in Table 1. The results of this basic characterization of the various

microalgae species are similar to those reported in the literature, for instance the results of Azazi et al. [31] and Zhao et al. [70] for CV; Batista et al. [71] and Zhao et al. [70] for IG; Sanchez-Silva et al. [72] and Lopez-Gonzalez et al. [73] for NG; Chen et al. [74] for NL; Bagnoud-Velásquez et al. [75] for PT; or Gai et al. [23] and Chen et al. [74] for SP.

Table 1: Results of basic characterization of the microalgae from 3 different tests with deviations below +/-1.5% (PA: Proximate Analysis, UA: Ultimate Analysis, VM: Volatile Matter, A: Ash, C: Carbon, H: Hydrogen, N: Nitrogen, S: Sulfur, HHV: High Heating Value, d: dry, daf: dry ash free, CV: *Chlorella Vulgaris*, IG: *Isochrysis Galbana*, NG: *Nannochloropsis Gaditana*, NL: *Nannochloropsis Limnetica*, PT: *Phaeodactylum Tricornutum*, SP: *Spirulina Platensis*).

		CV	**IG**	**NG**	**NL**	**PT**	**SP**
PA	VM [%d]	76.26	86.13	84.06	81.56	62.10	81.46
	A [%d]	13.11	8.31	10.52	9.16	25.46	6.40
UA	C [% daf]	59.06	47.60	58.62	58.13	54.53	53.12
	H [% daf]	8.81	7.22	9.01	8.59	8.87	7.84
	N [% daf]	11.39	5.97	8.81	9.06	9.14	12.34
	S [% daf]	0.66	0.89	0.69	0.56	1.94	0.74
	O* [% daf]	20.08	38.32	22.87	23.66	25.52	25.96
HHV [%d]		22.88	19.97	23.51	24.50	19.34	22.62

The microalgae species' carbohydrate, protein and lipid contents, as measured by several authors, are included in Table 2. Similar compositions are reported in the literature for CV, IG, NG and NL, for which the maximum content corresponds to proteins, whereas the carbohydrates content was the lowest. In contrast, SP is characterized by a very low content of lipids compared to other microalgae [76, 77, 78] and the contents of the three main components of microalgae, i.e., carbohydrates, proteins and lipids, are similar for PT [79].

Table 2: Contents of carbohydrates, proteins and lipids of various microalgae species obtained from the literature (CV: *Chlorella Vulgaris*, IG: *Isochrysis*

Galbana, NG: *Nannochloropsis Gaditana*, NL: *Nannochloropsis Limnetica*, PT: *Phaeodactylum Tricornutum*, SP: *Spirulina Platensis*).

	Carbohydrates [%]	Proteins [%]	Lipids [%]	References
CV	8.38-17.7	42.0-52.9	19.8-34.8	[80]
	8.8-16.6	47.1-58.8	10.4-21.6	[81]
	12.4	58.1	13.5	[73]
	12-17	51-58	14-22	[76]
IG	9.9±1.2	42.3±1.2	25.3±0.2	[82]
NG	12	37	33	[83]
	25.1	40.5	26.3	[73]
NL	10	37	24	[83]
PT	30±2	41±3	29±2	[79]
SP	8-14	46-63	4-9	[76]
	19.3	64.7	4.8	[77]
	19	60	6	[78]

4. Methodology

The pyrolysis measurements for the 6 microalgae species were conducted in a TGA Q500 thermogravimetric analyzer from TA Instruments. During the TGA tests, two processes were performed: the sample was dried completely at 105 ºC for 30 min and the temperature was reduced to 50 °C to investigate the pyrolysis of the sample when increasing the temperature of the TGA furnace to 800 ºC at a constant heating rate in an inert atmosphere. The reduction of temperature to 50 ºC and the increase to 800 ºC guarantee a constant heating rate in the range from 150 ºC to 600 ºC, which is the temperature range of interest for the pyrolysis of all microalgae species. The complete absence of oxygen required during the pyrolysis process was ensured by supplying the furnace with a constant nitrogen flowrate of 60 mL/min. The constant heating rates selected to increase the

temperature during pyrolysis were 10, 13, 16, 19, 22, 25, 30, 35, and 40 K/min. According to Soria-Verdugo et al. [84], the use of nine different TGA pyrolysis curves, obtained at nine different heating rates, provides accurate values for the kinetic parameters of the pyrolysis process, i.e., the activation energy *E* and the pre-exponential factor *A*. The selected heating rates ranged from 10 to 40 K/min to guarantee negligible effects of heat and mass transfer inside the sample, and the interval between heating rates increased for higher heating rates to improve visualization of the Arrhenius plots obtained for the different kinetic models, where a function of the logarithm of the heating rate is normally represented on the y-axis. Although the heating rates employed in the TGA pyrolysis experiments were low compared to those obtained in industrial applications, similar results were obtained by Soria-Verdugo et al. [85] in pyrolysis tests with the same TGA instrument for heating rates as high as 200 K/min.

During an isothermal process, the TGA Q500 temperature accuracy is ±1 ºC and the temperature precision is ±0.1 ºC. The weighing precision of the TGA is ±0.01% and its mass measurement sensitivity is 0.1 μg. The dynamic baseline drift during a heating process for an empty platinum pan from 50 ºC to 1000 ºC at 20 K/min is lower than 50 μg with no baseline subtraction. During pyrolysis measurements in the TGA, the mass of the microalgae samples was selected as 10.0 ± 0.5 mg, with a particle size under 100 μm, to reduce heat transfer effects in the sample [86, 87, 88]. The pyrolysis tests for each microalgae species and for each heating rate were conducted three times to guarantee the repeatability of the process, obtaining differences below 1%. A blank experiment was also run for each heating rate to exclude buoyancy effects [89].

5. Results and Discussion

5.1. TGA pyrolysis measurements

The evolution of the conversion α during pyrolysis can be obtained directly from measurement of the sample mass in the TGA. The conversion α for a range of temperatures from 150 ºC to 600 ºC, for the six different microalgae species analyzed is depicted in Figure 1. For each species, nine different heating rates were employed to increase the temperature during pyrolysis in the TGA. No analysis of the microalgae drying process was performed, and the pyrolysis conversion rate below 150 °C is negligible. Figure 1 shows that, for all microalgae species, an increase in the heating rate of the sample caused displacement of pyrolysis conversion to higher temperatures due to non-isothermal pyrolysis reactions [90, 91]. The TGA curves shown in Figure 1 for CV, IG, NG, and NL are quite similar, showing a maximum variation of the conversion in a temperature range between 250 ºC and 450 ºC. The similarities found for the TGA curves of these four microalgae species can be explained by their similar contents of carbohydrates, proteins and lipids. In contrast, the pyrolysis of PT begins at a lower temperature, at approximately 150 ºC, which indicates the presence of highly volatile components in this type of microalgae, which are associated with their high carbohydrate content. For SP, the TGA curve is smooth at the beginning of the pyrolysis. Then, pyrolysis is accelerated at a temperature of approximately 300 ºC, showing a sharp increase in the conversion due to the high content of proteins for this microalgal biomass, compared to their low contents of carbohydrates and lipids.

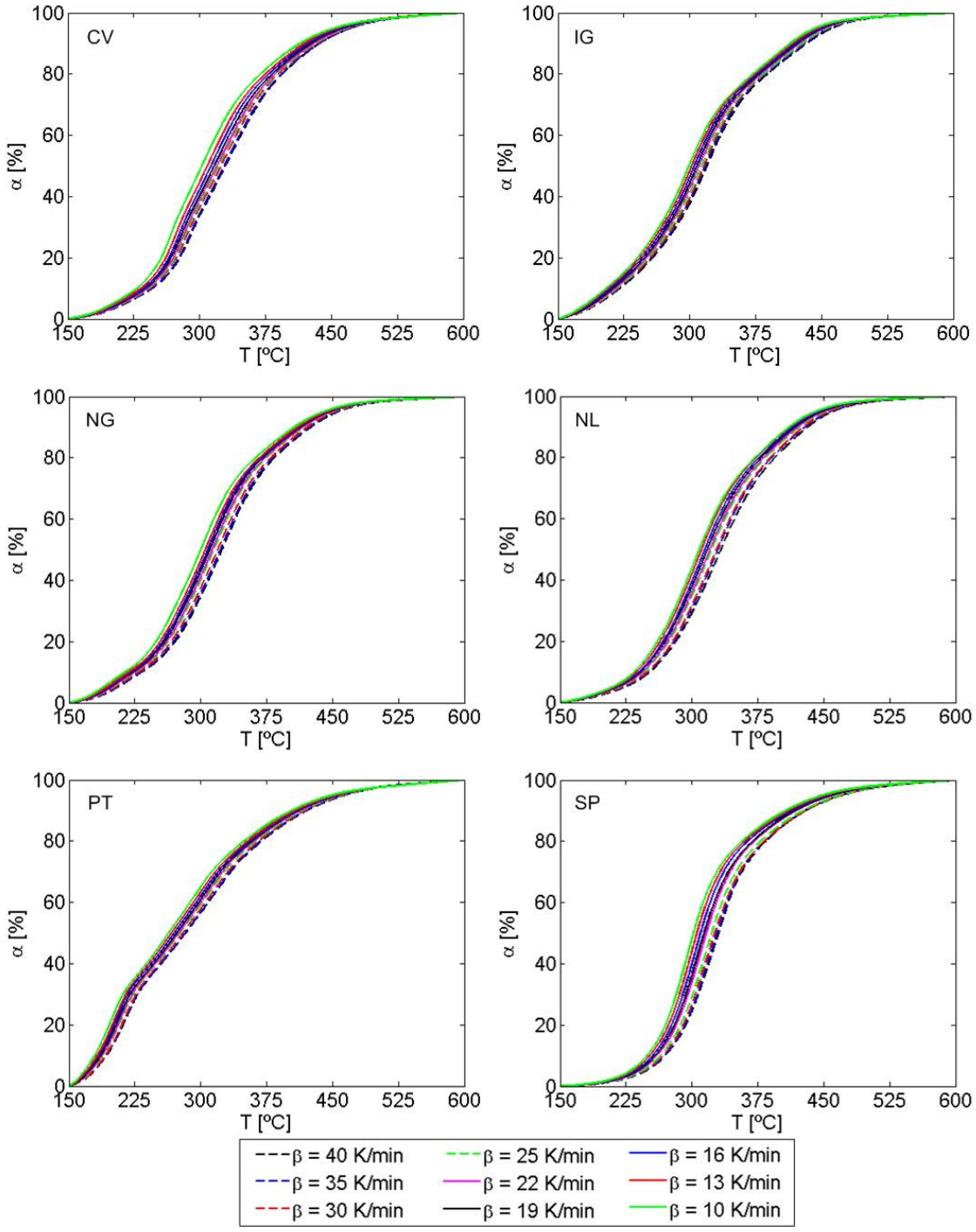

Figure 1: Evolution of conversion α with temperature T for various heating rates β from three tests obtaining deviations below +/-1% (CV: *Chlorella Vulgaris*, IG: *Isochrysis Galbana*, NG: *Nannochloropsis Gaditana*, NL: *Nannochloropsis Limnetica*, PT: *Phaeodactylum Tricornutum*, SP: *Spirulina Platensis*).

The comparison of the results of the pyrolysis tests conducted in the TGA for the various microalgae species can be performed more easily based on the DTG curves, where the rate of reaction, i.e., the derivative of the conversion with time,

$d\alpha/dt$, is plotted as a function of temperature T. The DTG curves of the various microalgae species are presented in Figure 2. An increase in the heating rate during pyrolysis causes a higher rate of reaction for all samples tested, as observed in Figure 2. Some similarities are still observed in the DTG curves of CV, IG, NG, and NL, both in the width of the curve and the values of the rate of reaction, due to their similar carbohydrate, protein and lipid contents. However, two different peaks are observed close to the maximum of the rate of reaction in the case of the CV sample, for which the maximum rate of reaction was attained for temperatures slightly below 300 ºC, whereas for the samples of IG, NG, and NL the maximum rate of reaction was reached at temperatures slightly above 300 ºC. The DTG curve of the PT is wider, covering a higher range of temperatures, and the values of the rate of reaction in this case are significantly lower than for the other microalgae species studied. This wider temperature range for the decomposition of PT is caused by similar contents of carbohydrates, for which decomposition is associated with low temperatures; proteins, which are decomposed at medium temperatures; and lipids, which undergo pyrolysis at higher temperatures [21]. Moreover, the maximum rate of reaction for the PT sample is achieved at a low temperature of approximately 200 ºC, which can be attributed to their high carbohydrate content compared to other microalgae species (Table 2). The highest reaction rates are obtained for SP, for which the DTG curve is narrower due to low contents of carbohydrates and lipids compared to proteins.

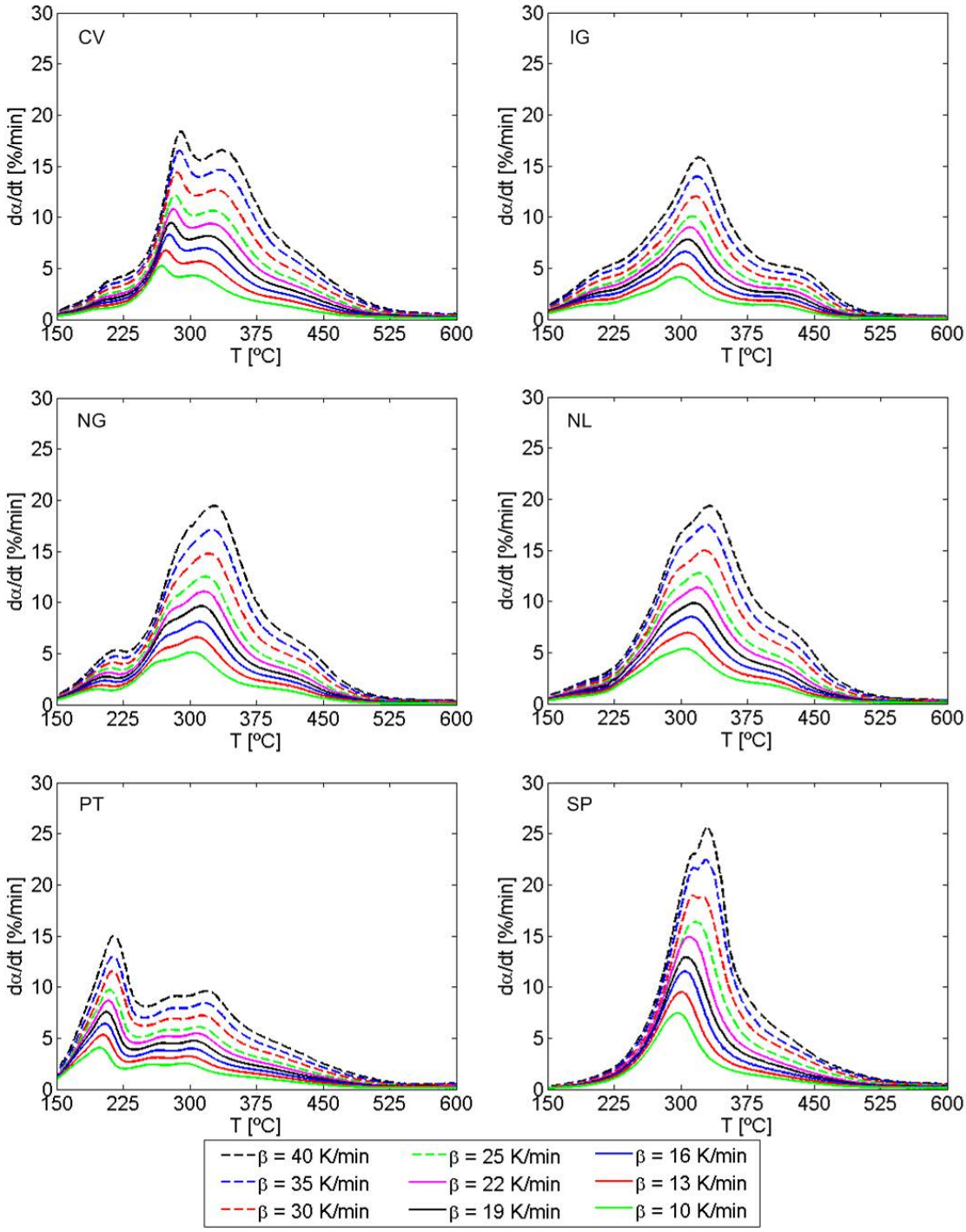

Figure 2: Evolution of conversion rate dα/dt with temperature T for various heating rates β (CV: *Chlorella Vulgaris*, IG: *Isochrysis Galbana*, NG: *Nannochloropsis Gaditana*, NL: *Nannochloropsis Limnetica*, PT: *Phaeodactylum Tricornutum*, SP: *Spirulina Platensis*).

5.2. Kinetic parameters for pyrolysis of microalgae

4.2.1. Arrhenius plots

Most methods described in the pyrolysis kinetics section are based on Arrhenius equations to obtain the kinetic parameters of the pyrolysis reaction, i.e., the activation energy *E* and the pre-exponential factor *A*. Considering the Arrhenius equations, Arrhenius plots can be built using the experimental data obtained from pyrolysis measurements conducted in the TGA at various heating rates.

5.2.1.1. Friedman method

In light of the Arrhenius equation obtained for the Friedman method, Eq. (7), the Friedman Arrhenius plot represents, for each heating rate, the values of $Ln(d\alpha/dt)$ versus $1/T$ for specific values of the conversion α. According to Eq. (7), the values presented in this Arrhenius plot for specific values of the conversion α, varying the heating rate β, should follow a linear trend. In fact, the activation energy can be directly obtained for each conversion as a function of the slope m_L of this linearization:

$$E = -m_L R. \tag{13}$$

Furthermore, the pre-exponential factor *A* can be determined from Eq. (7) for each conversion as a function of the intercept n_L of the linearization of the data presented in the Arrhenius plot:

$$A = \frac{\exp(n_L)}{(1-\alpha)}. \tag{14}$$

The Friedman Arrhenius plots for the microalgae species studied are shown in Figure 3, where the proper linearity of the data obtained for different heating rates can be observed.

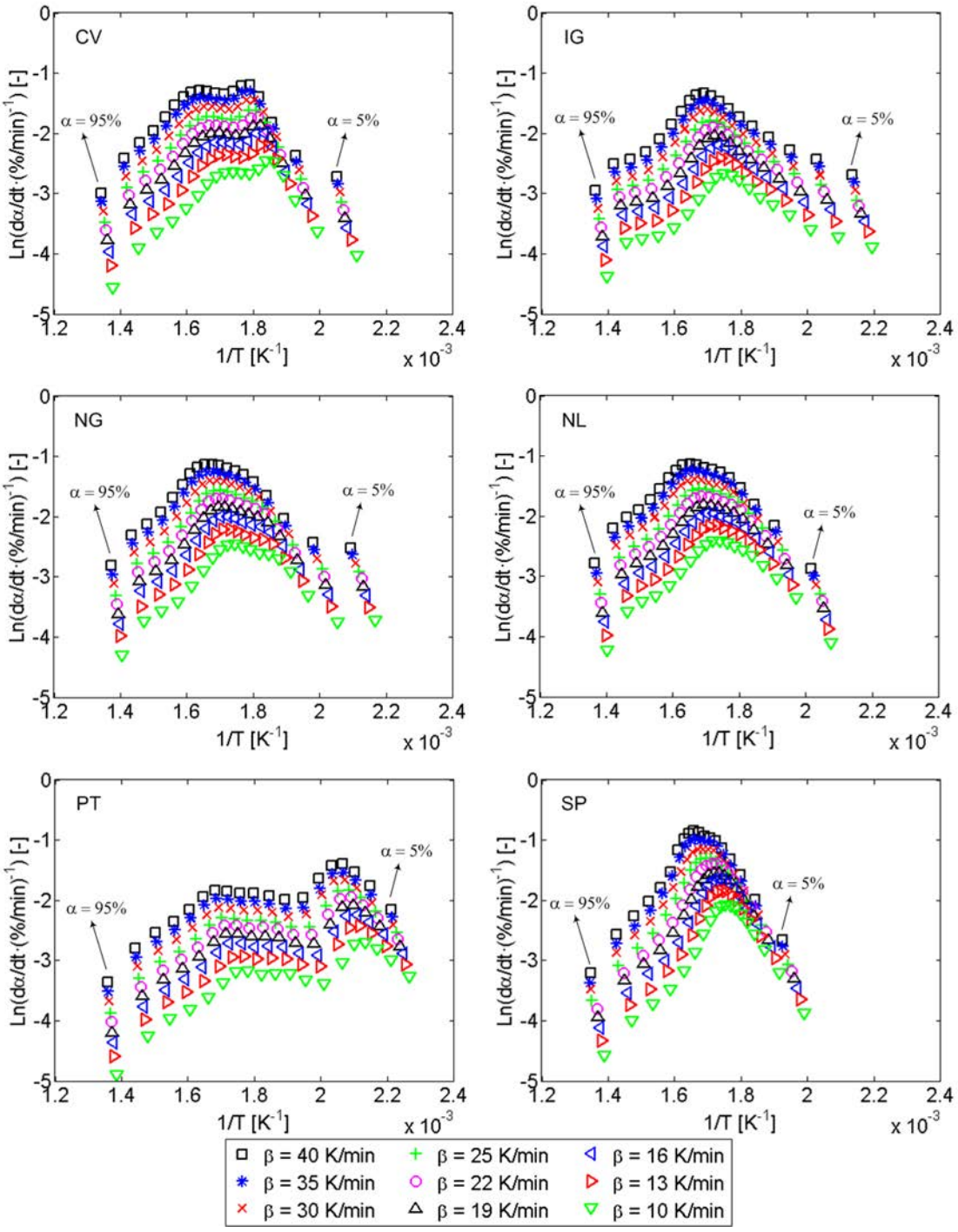

Figure 3: Friedman Arrhenius plots, logarithm of conversion rate dα/dt versus inverse temperature T for various heating rates β (data shown in intervals of conversion α of 5%) (CV: *Chlorella Vulgaris*, IG: *Isochrysis Galbana*, NG:

Nannochloropsis Gaditana, NL: *Nannochloropsis Limnetica*, PT: *Phaeodactylum Tricornutum*, SP: *Spirulina Platensis*).

5.2.1.2. OFW method

The Arrhenius equation of the OFW method is Eq. (8), in which a linear relationship between *Ln*(β) and *1/T* can be observed. Therefore, the OFW Arrhenius plot is built by representing, for specific values of the conversion α, the values of *Ln*(β) versus *1/T*. By linearizing the values shown in this OFW Arrhenius plot for each conversion and varying the heating rate, the slope m_L allows the calculation of the activation energy *E* for each value of the conversion as follows:

$$E = -\frac{m_L R}{1.052}. \quad (15)$$

However, for the calculation of the pre-exponential factor *A* from the linearization of the data presented in the OFW Arrhenius plot, an assumption for the form of *g(α)* should be made. Assuming first-order reactions, the form of the function is *g(α) = - Ln(1-α)* [18], and the pre-exponential factor can be obtained for each value of the conversion, from the slope m_L and intercept n_L of the linear fitting:

$$A = -\frac{1.052}{m_L}\left[-Ln\left(1-\alpha\right)\right]\exp\left(n_L + 5.3305\right). \quad (16)$$

Figure 4 shows the OFW Arrhenius plots for the various species of microalgae tested, indicting a good linearity of the data obtained for different heating rates.

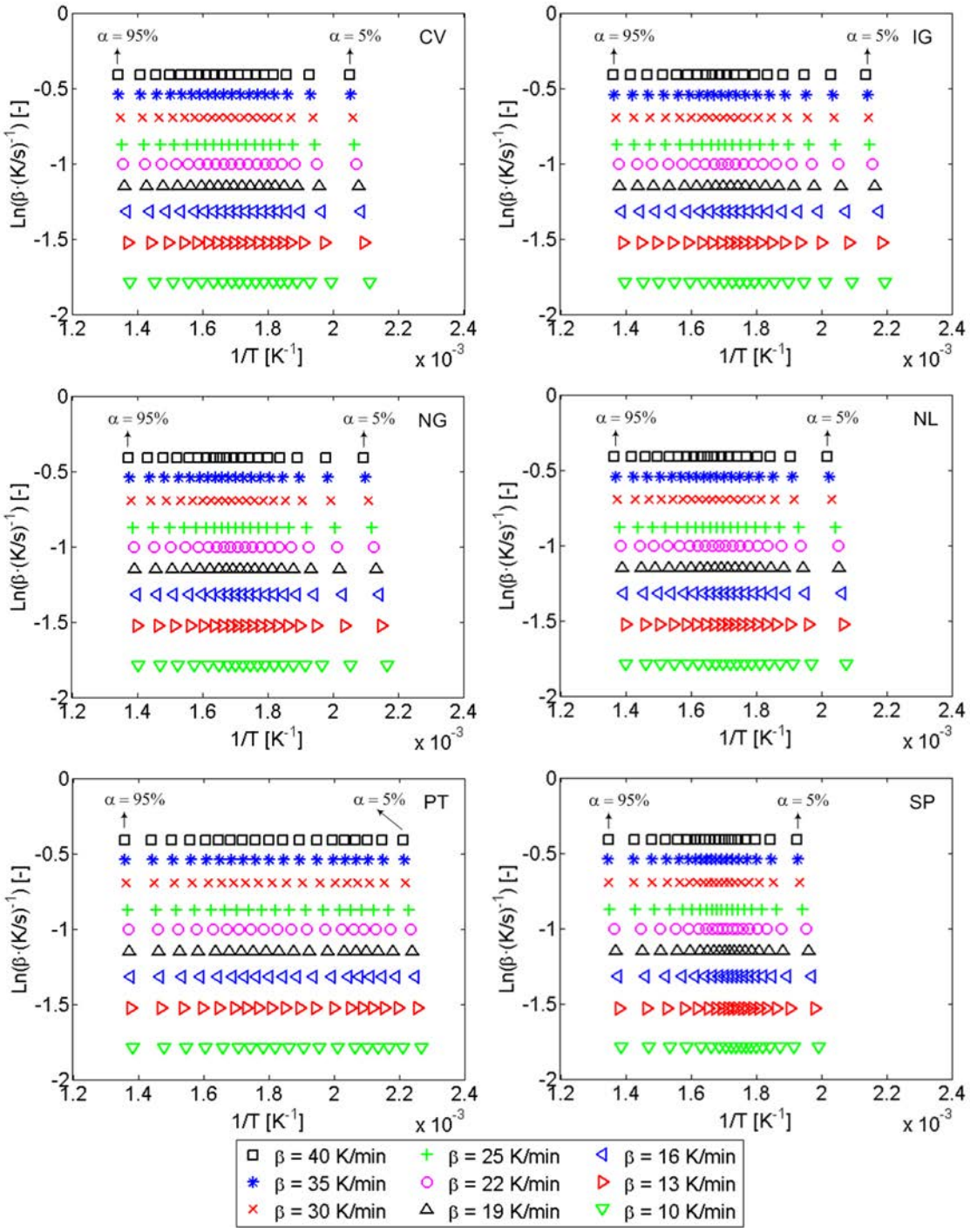

Figure 4: OFW Arrhenius plots, logarithm of heating rates β versus inverse temperature *T* (data shown in intervals of conversion α of 5%) (CV: *Chlorella Vulgaris*, IG: *Isochrysis Galbana*, NG: *Nannochloropsis Gaditana*, NL: *Nannochloropsis Limnetica*, PT: *Phaeodactylum Tricornutum*, SP: *Spirulina Platensis*).

5.2.1.3. KAS and simplified DAEM methods

Although the mathematical derivations of the methods KAS and simplified DAEM differ, the Arrhenius equations obtained in both cases, i.e., Eq. (9) for KAS and Eq. (11) for simplified DAEM, are quite similar. In both cases, a linear relationship of $Ln(\beta/T^2)$ with $1/T$ can be observed, and thus, their Arrhenius plots coincide, representing in both cases the values of $Ln(\beta/T^2)$ as a function of $1/T$ for specific conversion values. This Arrhenius plot is referred to as the KAS-DAEM Arrhenius plot. Both for KAS and simplified DAEM, the activation energy E can be obtained as a function of the slope m_L of the linearization of the data shown in the KAS-DAEM Arrhenius plot as follows:

$$E = -m_L R. \tag{17}$$

Nonetheless, since the Arrhenius equations of KAS, Eq. (9), and simplified DAEM, Eq. (11), are different, the calculation of the pre-exponential factor A from the linearization of the data represented in the KAS-DAEM Arrhenius plot differs for both methods. Applying the simplified DAEM, the pre-exponential factor can be calculated from the slope m_L and the intercept n_L of the linearization of the data in the KAS-DAEM Arrhenius plot:

$$A = -m_L \exp\left(n_L - 0.6075\right). \tag{18}$$

However, in light of Eq. (9), the calculation of the pre-exponential factor A applying KAS requires the assumption of the form of $g(\alpha)$. For first-order reactions, i.e., $g(\alpha) = -Ln(1-\alpha)$ [18], the pre-exponential factor can be obtained from the slope m_L and intercept n_L of the linear fitting as follows:

$$A = -m_L\left[-Ln\left(1-\alpha\right)\right]\exp\left(n_L\right). \tag{19}$$

The KAS-DAEM Arrhenius plots of the various microalgae species are presented in Figure 5, where again a proper linearity of the data can be seen.

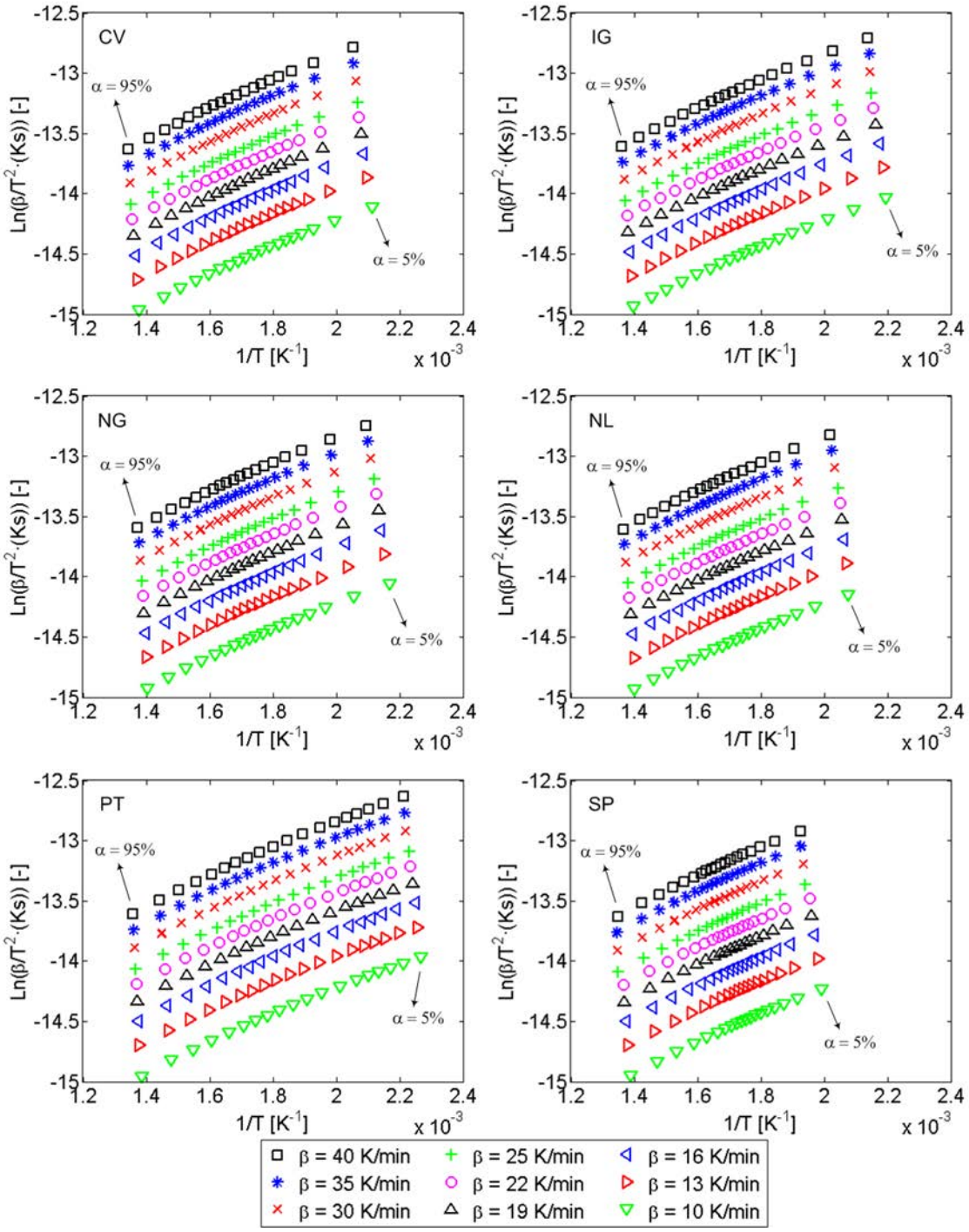

Figure 5: KAS-DAEM Arrhenius plots, logarithm of heating rate β over temperature squared T^2 versus inverse temperature T (data shown in intervals of conversion α of 5%) (CV: *Chlorella Vulgaris*, IG: *Isochrysis Galbana*, NG:

Nannochloropsis Gaditana, NL: *Nannochloropsis Limnetica*, PT: *Phaeodactylum Tricornutum*, SP: *Spirulina Platensis*).

5.2.1.4. Kissinger method

The Kissinger method is also based on an Arrhenius equation, Eq. (12), although in this case, only a single point is obtained for each heating rate curve, corresponding to the maximum rate of reaction. The Kissinger Arrhenius plot is built by plotting the values of $Ln(\beta/T_{max}^2)$ versus $1/T_{max}$, where T_{max} is the absolute temperature for which the DTG curve (Figure 2) shows a maximum. Nine points were obtained for each microalgae species, corresponding to the nine DTG curves measured by varying the heating rate during pyrolysis. The linearization of these nine points obtained for each sample permits the calculation of a unique value for both the activation energy E and the pre-exponential factor A. The value of the activation energy E is determined from the slope m_L of the linearization as follows:

$$E = -m_L R, \tag{20}$$

whereas the pre-exponential factor A can be calculated from Eq. (12) as a function of the slope m_L and the intercept n_L of the linear fitting as follows:

$$A = -m_L \exp\left(n_L\right). \tag{21}$$

The Kissinger Arrhenius plots of the six different species of microalgae analyzed are depicted together in Figure 6, showing the fair linearity of the data.

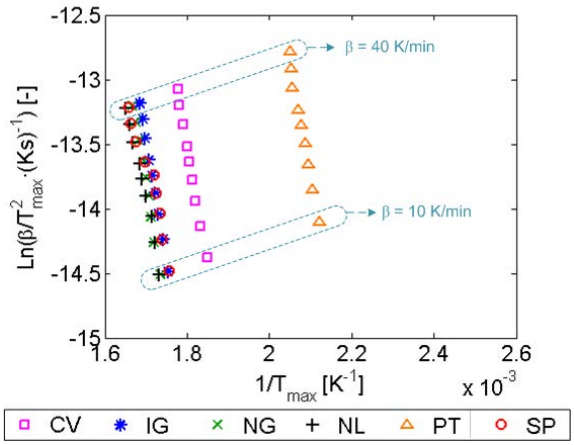

Figure 6: Kissinger Arrhenius plot, logarithm of heating rate β over the temperature of maximum conversion rate T_{max} versus inverse temperature of maximum conversion rate T_{max} (CV: *Chlorella Vulgaris*, IG: *Isochrysis Galbana*, NG: *Nannochloropsis Gaditana*, NL: *Nannochloropsis Limnetica*, PT: *Phaeodactylum Tricornutum*, SP: *Spirulina Platensis*).

The average values of the determination coefficient R^2 of the linear fitting of the data presented in the Arrhenius plots, for a range of conversions between 5% and 95% in intervals of 1%, are reported in Table 3. The high values of R^2 obtained for all microalgae species and kinetic methods tested indicate the high accuracy of the pyrolysis measurements conducted in the TGA [39]. No determination coefficient is reported for the Vyazovkin method since this method is not based on an Arrhenius plot. Furthermore, the linearization of the data shown in the different Arrhenius plots was also analyzed without considering the data obtained for the two highest heating rates, i.e., 35 and 40 K/min, to quantify the importance of heat and mass transfer effects inside the sample. Since negligible variations in the average R^2 values were obtained when the highest heating rates were not considered, the effects of heat and mass transfer inside the sample can be considered negligible for all tests.

Table 3: Average value of determination coefficient R^2 [-] for linearization of data shown in Arrhenius plots (CV: *Chlorella Vulgaris*, IG: *Isochrysis Galbana*, NG: *Nannochloropsis Gaditana*, NL: *Nannochloropsis Limnetica*, PT: *Phaeodactylum Tricornutum*, SP: *Spirulina Platensis*).

Microalgae	Friedman method	OFW method	KAS or DAEM method	Kissinger method
CV	0.992	0.990	0.989	0.994
IG	0.991	0.991	0.991	0.997
NG	0.992	0.993	0.992	0.986
NL	0.984	0.985	0.983	0.984
PT	0.993	0.994	0.994	0.986
SP	0.974	0.979	0.976	0.943

5.2.2. Activation energy and pre-exponential factor

The results obtained for the activation energy *E* and the pre-exponential factor *A* from the application of the various kinetic models tested on the six species of microalgae are shown in Figure 7 and Figure 8, respectively, for a range of conversions between 5% and 95% in intervals of 1%. No values for the pre-exponential factor *A* are reported for the Vyazovkin method in Figure 8, since the minimization of the function shown in Eq. (10) only permits the calculation of the activation energy *E*. A narrow range of variation of the kinetic parameters is obtained for the SP sample, for which the activation energy varies from 98.5 to 226.5 kJ/mol and the pre-exponential factor ranges from $7.8 \cdot 10^{6}$ to $5.8 \cdot 10^{15}$ s^{-1}, due to their low content of carbohydrates and lipids. A wider range of variation is found for the kinetic parameters of the samples of CV, IG, NG, and NL, for which the activation energies vary respectively in the ranges 135.6 – 337.1 kJ/mol, 148.4 – 309.4 kJ/mol, 137.4 – 373.0 kJ/mol, and 123.2 – 295.6 kJ/mol, whereas the pre-exponential factors are contained in the intervals $8.7 \cdot 10^{9}$ – $4.1 \cdot 10^{23}$ s^{-1}, $1.2 \cdot 10^{12}$ – $6.9 \cdot 10^{22}$ s^{-1}, $1.1 \cdot 10^{11}$ – $7.2 \cdot 10^{26}$ s^{-1}, and $1.1 \cdot 10^{9}$ – $1.5 \cdot 10^{21}$ s^{-1}, respectively. The ranges of *E* and *A* for these four microalgae are similar, due to their similar composition concerning carbohydrates, proteins and lipids. The largest range of variation for the kinetic parameters was obtained for the PT

sample, for which the activation energy varied from 145.0 to 452.2 kJ/mol, while the pre-exponential factor varied from $5.3 \cdot 10^{12}$ to $7.9 \cdot 10^{31}$ s^{-1}. The higher range of variation of *E* and *A* for PT can be attributed to their similar contents of carbohydrates, proteins and lipids. The values obtained here for the pyrolysis kinetic parameters are in the range typically found for microalgae in the literature. In particular, the values obtained for CV, which is the most commonly studied microalgae, are similar to those reported by Chen et al. [28], Kassim et al. [27], Ferreira et al. [92], Figueira et al. [93], Hu et al. [35], Yuan et al. [32], Zhao et al. [70], Maurya et al. [94], and Azazi et al. [31]. The results obtained for IG and NG are in agreement with those reported by Zhao et al. [70] and López-González et al. [73], respectively, whereas the kinetics parameters of PT and SP are comparable to the values stated by Bagnoud-Velásquez et al. [78] and Gai et al. [23]. The accurate values obtained for the pyrolysis kinetic parameters *E* and *A* for the different microalgae species tested, which were obtained from nine different TGA curves, can be employed to estimate the thermal degradation of these microalgae in various pyrolysis reactors. The kinetic models based on the kinetic parameters might be combined with a heat and mass transfer model to globally describe the pyrolysis process of microalgae samples. These combined kinetic-transport phenomena models constitute a magnificent tool to optimize the design of pyrolysis reactors to maximize the efficiency of the pyrolysis. Furthermore, the pyrolysis kinetic parameters reported in this work may even be used as a first approximation for different microalgae species, provided that the composition of the microalga is similar to those analyzed in this study.

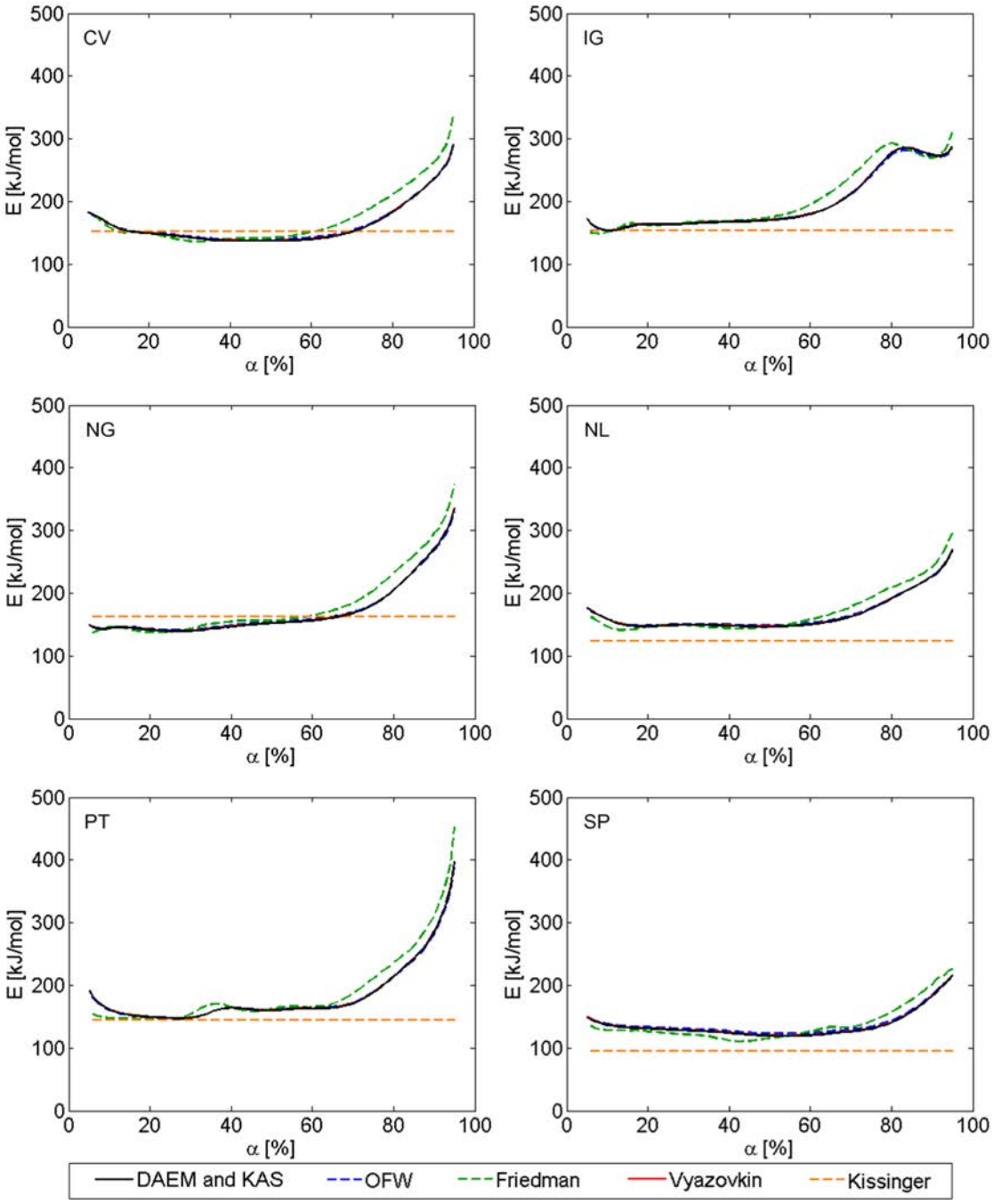

Figure 7: Activation energies *E* as a function of conversion α for six microalgae species applying various kinetic models (CV: *Chlorella Vulgaris*, IG: *Isochrysis Galbana*, NG: *Nannochloropsis Gaditana*, NL: *Nannochloropsis Limnetica*, PT: *Phaeodactylum Tricornutum*, SP: *Spirulina Platensis*).

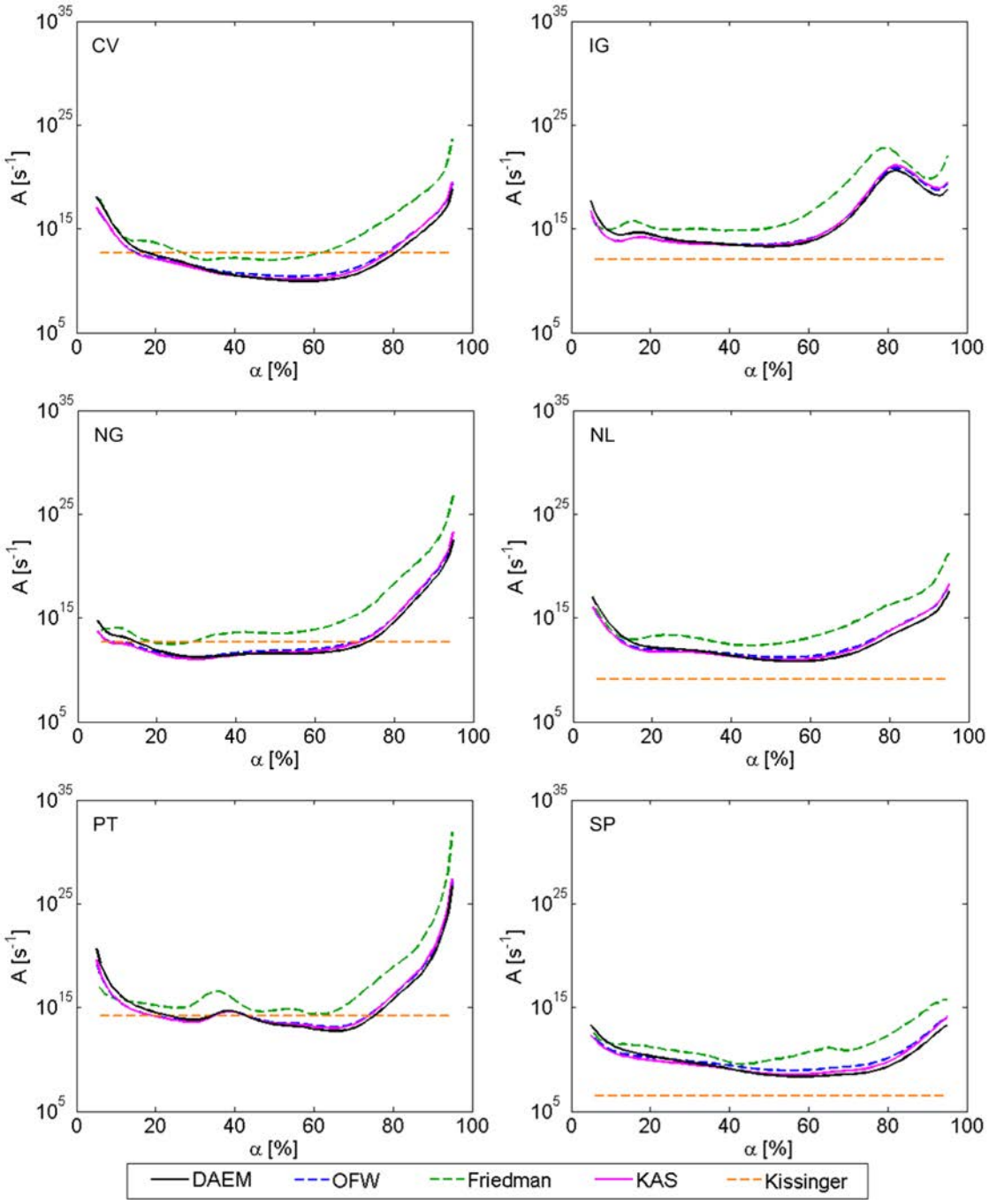

Figure 8: Pre-exponential factors *A* as a function of conversion α for six microalgae species applying various kinetic models (CV: *Chlorella Vulgaris*, IG: *Isochrysis Galbana*, NG: *Nannochloropsis Gaditana*, NL: *Nannochloropsis Limnetica*, PT: *Phaeodactylum Tricornutum*, SP: *Spirulina Platensis*).

Fairly good agreement can be observed for the results obtained using the simplified DAEM and the different integral isoconversional methods considered, i.e., the OFW, KAS and Vyazovkin methods. In contrast, deviations from these results were obtained when applying the differential isoconversional method of

Friedman or the method of Kissinger. A quantification of the deviations obtained for the kinetic parameters of each microalgae species, determined by applying the different kinetic methods tested, is seen in Tables 4 and 5, where the average relative error for the activation energies and the logarithm of the pre-exponential factors obtained is reported. For calculation of these relative errors, the results obtained for the kinetic parameters applying the simplified DAEM are considered as a base case, comparing the parameters derived from the other kinetic methods to those determined by the simplified DAEM.

Table 4: Average relative error [%] for activation energy obtained with various kinetic methods compared to those determined by simplified DAEM (CV: *Chlorella Vulgaris*, IG: *Isochrysis Galbana*, NG: *Nannochloropsis Gaditana*, NL: *Nannochloropsis Limnetica*, PT: *Phaeodactylum Tricornutum*, SP: *Spirulina Platensis*).

Microalgae	Vyazovkin method	OFW Method	Friedman method	Kissinger method
CV	0.18	1.14	6.80	11.62
IG	0.12	0.48	4.31	18.05
NG	0.16	0.92	5.83	14.48
NL	0.18	0.92	4.86	23.91
PT	0.12	0.47	5.74	16.68
SP	0.24	2.12	6.63	28.79

Table 5: Average relative error [%] for logarithm of pre-exponential factor obtained using various kinetic methods compared to those determined by simplified DAEM (CV: *Chlorella Vulgaris*, IG: *Isochrysis Galbana*, NG: *Nannochloropsis Gaditana*, NL: *Nannochloropsis Limnetica*, PT: *Phaeodactylum Tricornutum*, SP: *Spirulina Platensis*).

Microalgae	KAS method	OFW Method	Friedman method	Kissinger method
CV	2.71	3.63	18.23	16.51
IG	2.19	1.99	11.73	20.14
NG	2.58	2.74	16.40	11.68
NL	2.68	3.22	14.82	26.17
PT	2.22	2.31	12.23	9.78
SP	3.45	5.35	19.49	32.01

As observed in Tables 4 and 5, the values of the activation energies and pre-exponential factors obtained for the microalgae species using the Friedman and the Kissinger methods differ from those determined by applying the simplified DAEM, resulting in large average relative errors. For the Kissinger method, these discrepancies should be attributed to the limitation of this method, which employs only the information related to the maximum rate of reaction to obtain unique values for the activation energy and pre-exponential factor. The other kinetic methods calculate values of *E* and *A* that vary with the conversion α. The differential character of the Friedman method is known to result in a lower accuracy than integral isoconversional methods [18, 43]. In fact, the application of the integral isoconversional OFW and KAS methods to determine the kinetic parameters of the various microalgae species leads to lower average relative errors compared to the results determined by the simplified DAEM. The activation energy obtained from KAS and simplified DAEM coincide, as stated above, and thus no information about the relative error of the activation energy of KAS compared to that of simplified DAEM is included in Table 4, since this value is zero in all cases. For the application of the Vyazovkin method to determine the activation energies of the microalgae samples, the resulting values are very similar to those calculated from the simplified DAEM, obtaining a maximum average relative error of 0.24% for all microalgae species tested. Similar conclusions about the reliability of isoconversional kinetic models have been obtained for lignocellulosic biomass samples [39].

6. Conclusions

Pyrolysis of the microalgae *Chlorella Vulgaris* (CV), *Isochrysis Galbana* (IG), *Nannochloropsis Gaditana* (NG), *Nannochloropsis Limnetica* (NL), *Phaeodactylum Tricornutum* (PT), and *Spirulina Platensis* (SP) was investigated based on thermogravimetric measurements at nine different heating rates. CV, IG, NG, and NL show similar behavior during the pyrolysis for temperatures between 250 ºC and 450 ºC. In contrast, the range of temperatures in which the pyrolysis of PT occurs varies from 150 ºC to 450 ºC, whereas SP is characterized by a narrow pyrolysis temperature window near 300 ºC.

The TGA measurements conducted for all microalgae species were employed to analyze the kinetics of the pyrolysis process via application of several kinetic methods: Kissinger, Friedman, OFW, KAS, Vyazovkin, and simplified DAEM. The activation energies obtained from these methods for the microalgae species varied between 135.6 – 337.1 kJ/mol (CV), 148.4 – 309.4 kJ/mol (IG), 137.4 – 373.0 kJ/mol (NG), 123.2 – 295.6 kJ/mol (NL), 145.0 – 452.2 kJ/mol (PT), and 98.5 – 226.5 kJ/mol (SP). Regarding the pre-exponential factors determined by the kinetic models, variations between $8.7 \cdot 10^{9}$ – $4.1 \cdot 10^{23}$ s^{-1} (CV), $1.2 \cdot 10^{12}$ – $6.9 \cdot 10^{22}$ s^{-1} (IG), $1.1 \cdot 10^{11}$ – $7.2 \cdot 10^{26}$ s^{-1} (NG), $1.1 \cdot 10^{9}$ – $1.5 \cdot 10^{21}$ s^{-1} (NL), $5.3 \cdot 10^{12}$ – $7.9 \cdot 10^{31}$ s^{-1} (PT), and $7.8 \cdot 10^{6}$ – $5.8 \cdot 10^{15}$ s^{-1} (SP), were obtained. The results obtained for the pyrolysis kinetic parameters of the microalgae samples from the application of the different kinetic models for each conversion were compared to those determined by applying the simplified DAEM, with low discrepancies for the results of the integral isoconversional models, i.e., OFW, KAS, and Vyazovkin. However, moderate differences were found when comparing the kinetic parameters obtained from the simplified DAEM and those of the differential

isoconversional method of Friedman. Even higher discrepancies were found by comparing the unique values of the activation energies and pre-exponential factors calculated by the Kissinger method. Therefore, the use of the simplified DAEM or an integral isoconversional method, such as OFW, KAS or Vyazovkin, is recommended. The pyrolysis kinetic parameters obtained from the simplified DAEM or an integral isoconversional method may be used in combination with a heat and mass transfer model to globally describe the pyrolysis process of microalgae, permitting optimization of the pyrolysis reactor.

Appendix 1

In this appendix, the detailed mathematical derivation for various pyrolysis kinetic models is presented.

A1.1. Friedman method

The Friedman method [13] is a differential isoconversional method based on the differential form of the rate equation, Eq. (4). Applying logarithms to Eq. (4), the Arrhenius equation for the Friedman method can be obtained:

$$Ln\left(\frac{d\alpha}{dt}\right) = Ln\left(A \cdot f\left(\alpha\right)\right) - \frac{E}{RT}. \quad \text{(A1)}$$

The Friedman method is sometimes applied in combination with the assumption of a first order reaction, for which the form of the function *f* is $f(\alpha) = 1 - \alpha$. This assumption permits a simple calculation of the pre-exponential factor *A*, from the Arrhenius equation of the Friedman method for a first-order reaction:

$$Ln\left(\frac{d\alpha}{dt}\right) = Ln\left(A\left(1-\alpha\right)\right) - \frac{E}{RT}. \quad \text{(A2)}$$

A1.2. Ozawa-Flynn-Wall method

The Ozawa-Flynn-Wall method [14, 15] is an integral isoconversional method based on an approximation for the integral form of the rate equation, Eq. (6). The OFW method is based on a substitution method, for which a new variable *z* is defined as follows:

$$z = \frac{E}{RT}, \tag{A3}$$

resulting after differentiation in the following:

$$dT = -\frac{E}{Rz^2}dz. \tag{A4}$$

The integral form of the rate equation, Eq. (6), can be written on this new variable as follows:

$$g(\alpha) = \frac{A}{\beta}\int_0^T \exp\left(-\frac{E}{RT}\right)dT = \frac{AE}{\beta R}\int_z^\infty \exp(-z)\,z^{-2}dz. \tag{A5}$$

The integral over *z* on the right-hand side of Eq. (A5) is known as *p(z)*, which is the so-called temperature integral:

$$p(z) = \int_z^\infty \exp(-z)\,z^{-2}dz. \tag{A6}$$

With this definition of *p(z)*, Eq. (A5) now reads as follows:

$$g(\alpha) = \frac{AE}{\beta R}\,p(z), \tag{A7}$$

from which the heating rate can be written as follows:

$$\beta = \frac{AE}{Rg(\alpha)} p(z). \tag{A8}$$

Therefore, applying logarithms to Eq. (A8), an Arrhenius equation is obtained:

$$Ln(\beta) = Ln\left(\frac{AE}{Rg(\alpha)}\right) + Ln\left(p(z)\right). \tag{A9}$$

The OFW method uses the approximation of Doyle [44] for the logarithm of *p(z)*, which reads as follows:

$$Ln\left(p(z)\right) \approx -5.3305 - 1.052z. \tag{A10}$$

Using Doyle's approximation in Eq. (A9), the Arrhenius equation for the OFW method is obtained:

$$Ln(\beta) = Ln\left(\frac{AE}{Rg(\alpha)}\right) - 5.3305 - 1.052\frac{E}{RT}. \tag{A11}$$

A1.3. Kissinger-Akahira-Sunose method

The accuracy of the OFW method was improved by the Kissinger-Akahira-Sunose method [4, 16]. KAS is also an integral isoconversional method based on an approximation of the temperature integral, *p(z)*. In contrast to OZW, where Doyle's approximation is employed, KAS uses the approximation of Coats-Redfern [6]. According to Coats and Redfern [6], the temperature integral, *p(z)*, can be approximated as follows:

$$p(z) = \int_z^\infty \exp(-z) z^{-2} dz \approx z^{-1} \exp(-z) \sum_{n=0}^{\infty} \frac{(-1)^n 2^n}{z^{n+1}}. \tag{A12}$$

Considering the definition of the variable *z,* Eq. (A3), and the temperature integral *p(z),* Eq. (A12), the integral of the right-hand side of the integral form of the rate equation, Eq. (6), can be approximated as follows:

$$\int_0^T \exp\left(-\frac{E}{RT}\right)dT = \frac{E}{R}\,p(z) \approx T\exp\left(-\frac{E}{RT}\right)\left[\frac{RT}{E} - \frac{2R^2T^2}{E^2} + \ldots\right]. \tag{A13}$$

For typical values of the absolute temperatures *T* and activation energies *E* obtained during the pyrolysis of solid fuels, the integral can be properly approximated using only the first term of the summation, obtaining the approximation of Coats-Redfern, which is valid for high values of $z = E/RT$:

$$\int_0^T \exp\left(-\frac{E}{RT}\right)dT \approx \frac{RT^2}{E}\exp\left(-\frac{E}{RT}\right). \tag{A14}$$

Using the approximation of Coats-Redfern in Eq. (6):

$$g(\alpha) = \frac{A}{\beta}\frac{RT^2}{E}\exp\left(-\frac{E}{RT}\right), \tag{A15}$$

and rearranging the terms to

$$\frac{\beta}{T^2} = \frac{AR}{Eg(\alpha)}\exp\left(-\frac{E}{RT}\right), \tag{A16}$$

we finally yield the Arrhenius equation for the KAS method by applying logarithms:

$$Ln\left(\frac{\beta}{T^2}\right) = Ln\left(\frac{AR}{Eg(\alpha)}\right) - \frac{E}{RT}. \tag{A17}$$

A1.4. Vyazovkin method

The Vyazovkin method [17] is also an integral isoconversional method that intends to increase the accuracy of the approximation of the temperature integral, *p(z)*. Vyazovkin and Dollimore [17] introduced the function *I(E,T)*:

$$I(E,T) = \int_0^T \exp\left(-\frac{E}{RT}\right) dT, \tag{A18}$$

so that, the integral form of the rate equation, Eq. (6), can be written simply as:

$$g(\alpha) = \frac{A}{\beta} I(E,T). \tag{A19}$$

Therefore, according to the isoconversional principle, which establishes that the reaction model is independent of the heating rate, the values of $g(\alpha)$ for the same values of the conversion α must coincide even for different heating rates β_j (with j = 1, 2, …, N, with N being the total number of different heating rates analyzed):

$$\frac{A_\alpha}{\beta_1} I\left(E_\alpha, T_{\alpha,1}\right) = \frac{A_\alpha}{\beta_2} I\left(E_\alpha, T_{\alpha,2}\right) = \ldots = \frac{A_\alpha}{\beta_N} I\left(E_\alpha, T_{\alpha,N}\right), \tag{A20}$$

where the values of the pre-exponential factor A_α and the activation energy E_α are exclusive functions of the conversion α, whereas the absolute temperature $T_{\alpha,j}$ depends on both the conversion α and the heating rate β_j. From the fulfillment of Eq. (A20), it follows that:

$$\sum_{i=1}^{N} \sum_{j=1}^{N} \frac{I\left(E_\alpha, T_{\alpha,i}\right)/\beta_i}{I\left(E_\alpha, T_{\alpha,j}\right)/\beta_j} = N(N-1) \qquad (\text{with } i \neq j). \tag{A21}$$

However, the values of $T_{\alpha,j}$ will be measured subject to some experimental error and, thus, Eq. (A21) can only be satisfied as an approximate equality.

Consequently, the activation energy for each conversion, E_α, can be obtained from the condition of the minimum value:

$$\left| N(N-1) - \sum_{i=1}^{N} \sum_{j=1}^{N} \frac{I\left(E_\alpha, T_{\alpha,i}\right)/\beta_i}{I\left(E_\alpha, T_{\alpha,j}\right)/\beta_j} \right| = \min \qquad (\text{with } i \neq j). \tag{A22}$$

The values of the integral $I(E_\alpha, T_{\alpha,j})$ could be computed numerically, but this would be a very time-consuming procedure [17]. Therefore, instead of a numerical solution of the integral, the Vyazovkin method is also based on an approximation for the temperature integral, $p(z)$, which is related to $I(E_\alpha, T_{\alpha,j})$ as follows:

$$I(E,T) = \frac{E}{R} p(z). \tag{A23}$$

In contrast to OFW and KAS, the Vyazovkin method employs the approximation of Senum-Yang [45] for the temperature integral, $p(z)$:

$$p(z) \approx \frac{\exp(-z)}{z} \frac{z^2 + 10z + 18}{z^3 + 12z^2 + 36z + 24}. \tag{A24}$$

The approximation of Senum-Yang for $p(z)$ is more accurate than those of Doyle and Coats-Redfern. In fact, using the Senum-Yang approximation, a limited deviation of 0.02% from the exact value of the temperature integral is obtained even for values of z as low as 5. Using the approximation of Senum-Yang, accurate values for the activation energy E_α can be obtained from the minimization equation, Eq. (A22), with reduced computational cost.

A1.5. Simplified Distributed Activation Energy Model

The Distributed Activation Energy Model was originally proposed by Vand [10] as a multi-step model to describe the chemical kinetics of solid fuel reactions. The

original method was simplified later by Miura [46], and Miura and Maki [47] derived in an integral method generally known as simplified DAEM. The simplified DAEM method assumes that the chemical kinetics of a complex solid fuel is governed by a large number of pseudo-components, each comprised of a theoretical infinite number of chemical reactions, sharing the same pre-exponential factor, but with a different activation energy following a distribution *f(E)*. According to DAEM, all chemical reactions occurring during the thermal degradation of a solid fuel are first-order, and the integral form of the rate equation, Eq. (6), can be written, for a known range of activation energies between *E* and *E* + *dE*, as follows:

$$\int_0^{\alpha} \frac{d\alpha\left(E, E+dE\right)}{\left(1-\alpha\left(E, E+dE\right)\right)} = \frac{A}{\beta}\int_0^{T} \exp\left(-\frac{E}{RT}\right) dT. \tag{A25}$$

By integrating the left-hand side of Eq. (A25), the conversion α*(E,E+dE)* for this activation energy range can be expressed as:

$$\alpha\left(E, E+dE\right) = 1-\exp\left[-\frac{A}{\beta}\int_0^{T} \exp\left(-\frac{E}{RT}\right) dT\right]. \tag{A26}$$

The overall value of the conversion α will be obtained by integrating over the whole possible interval of activation energies, considering the probability density function of the activation energies to be *f(E)*:

$$\alpha = 1-\int_0^{\infty} \exp\left[-\frac{A}{\beta}\int_0^{T} \exp\left(-\frac{E}{RT}\right) dT\right] f\left(E\right) dE. \tag{A27}$$

The exponential function in Eq. (A27) is the so-called ϕ function:

$$\phi(E,T) = \exp\left[-\frac{A}{\beta}\int_0^T \exp\left(-\frac{E}{RT} \right) dT \right]. \quad \text{(A28)}$$

Using the approximation of Coats-Redfern, Eq. (A14), the ϕ function can be simplified to:

$$\phi(E,T) \approx \exp\left[-\frac{ART^2}{\beta E}\exp\left(-\frac{E}{RT} \right) \right]. \quad \text{(A29)}$$

Considering the rapid variation of the ϕ function, it is typically approximated as a step function for a value $E = E_a$. Therefore, the conversion α, described by Eq. (A27) can be written based on this simplification for the ϕ function as follows:

$$\alpha = 1 - \int_0^\infty \phi(E,T)\, f(E)\, dE \approx 1 - \int_{E_a}^\infty f(E)\, dE = \int_0^{E_a} f(E)\, dE, \quad \text{(A30)}$$

where the normalization condition for the probability density function *f(E)* was employed in the last equality. Miura [46] analyzed the effect of the simplification of the ϕ function as a step function, concluding that a value of $\phi(E,T)$ = 0.58 is valid for solid fuels with a broad range of activation energies and pre-exponential factors. Using this value in the definition of the function ϕ, simplified according to the Coats-Redfern approximation, Eq. (A29) results in the following:

$$\phi(E,T) = 0.58 \approx \exp\left[-\frac{ART^2}{\beta E}\exp\left(-\frac{E}{RT} \right) \right]. \quad \text{(A31)}$$

Applying logarithms in Eq. (A31) and rearranging terms, the Arrhenius equation for the simplified DAEM method is obtained:

$$Ln\left(\frac{\beta}{T^2} \right) = Ln\left(\frac{AR}{E} \right) + 0.6075 - \frac{E}{RT}. \quad \text{(A32)}$$

A1.6. Kissinger method

The Kissinger method [4, 5] is based on the differential form of the rate equation, Eq. (4), assuming a generic order *n* for the chemical reaction, i.e., $f(\alpha) = (1-\alpha)^n$:

$$\frac{d\alpha}{dt} = A\exp\left(-\frac{E}{RT}\right)(1-\alpha)^n. \tag{A33}$$

When a solid sample is subjected to a temperature increase, the rate of reaction, $d\alpha/dt$, reaches a maximum for an absolute temperature T_{max}, that is as follows:

$$\frac{d}{dt}\left(\frac{d\alpha}{dt}\right) = 0 \Leftrightarrow T = T_{\max}. \tag{A34}$$

An expression for the derivative of the rate of reaction can be found by applying the chain rule as:

$$\frac{d}{dt}\left(\frac{d\alpha}{dt}\right) = \frac{d\alpha}{dt}\frac{d}{d\alpha}\left(A(1-\alpha)^n\right)\exp\left(-\frac{E}{RT}\right) + \frac{dT}{dt}\frac{d}{dT}\left(\exp\left(-\frac{E}{RT}\right)\right)A(1-\alpha)^n. \tag{A35}$$

After rearranging terms in Eq. (A35), the variation of the rate of reaction can be expressed as follows:

$$\frac{d}{dt}\left(\frac{d\alpha}{dt}\right) = \frac{d\alpha}{dt}\left[\frac{E\beta}{RT^2} - An(1-\alpha)^{n-1}\exp\left(-\frac{E}{RT}\right)\right]. \tag{A36}$$

Therefore, the temperature T_{max} for which the rate of reaction is maximal must fulfill the following:

$$\frac{E\beta}{RT_{\max}^2} = An(1-\alpha)^{n-1}\exp\left(-\frac{E}{RT_{\max}}\right), \tag{A37}$$

resulting in

$$\frac{\beta}{T_{\max}^2} = \frac{AR}{E} n\left(1-\alpha\right)^{n-1} \exp\left(-\frac{E}{RT_{\max}}\right). \quad \text{(A38)}$$

The Arrhenius equation for the Kissinger method is obtained after applying logarithms to Eq. (A38) to give a generic reaction order *n* for the chemical reactions [5]:

$$Ln\left(\frac{\beta}{T_{\max}^2}\right) = Ln\left(\frac{AR}{E} n\left(1-\alpha\right)^{n-1}\right) - \frac{E}{RT_{\max}}. \quad \text{(A39)}$$

This equation can be further simplified assuming first-order chemical reactions, i.e. $n = 1$, resulting in [4]:

$$Ln\left(\frac{\beta}{T_{\max}^2}\right) = Ln\left(\frac{AR}{E}\right) - \frac{E}{RT_{\max}}. \quad \text{(A40)}$$

Acknowledgments

The authors express their gratitude to the BIOLAB experimental facility. Funding by Deutsches Zentrum für Luft- und Raumfahrt e. V. (DLR), the German Aerospace Center, is gratefully acknowledged as well as funding by the DLR international collaboration project “Accurate Kinetic Data of Biomass Pyrolysis”.

Declaration of authors contribution

The experimental measurements of the pyrolysis of the various microalgae species were conducted in the Carlos III University of Madrid (Spain) by Prof. Antonio Soria-Verdugo and Prof. Nestor García-Hernando. The kinetic models were implemented by Prof. Antonio Soria-Verdugo, Dr Elke Goos, and Prof. Uwe Riedel, during a summer research stay of Prof. Antonio Soria-Verdugo in the

German Aerospace Center (DLR) in Stuttgart (Germany). Finally, all the authors contributed in the discussion of the results and writing the paper.

Conflict of interests

The authors declare that there are no potential, financial or other interests that could be perceived to influence the outcomes of this research.

Informed Consent (Human/Animal Rights)

No conflicts, informed consent, human or animal rights applicable.

Declaration of authors agreement

The authors declare their agreement to authorship and submission of the manuscript for peer review.

References

[1] Marcilla A., Catalá L., García-Quesada J.C., Valdés F.J., Hernández M.R. A review of thermochemical conversion of microalgae. Renew. Sust. Energ. Rev. 2013; 27, 11-19.

[2] Ceylan S., Kazan D. Pyrolysis kinetics and thermal characteristics of microalgae Nannochloropsis oculata and Tetraselmis sp. Bioresour. Technol. 2015; 187, 1-5.

[3] Bhavanam A., Sastry R.C. Kinetic study of solid waste pyrolysis using distributed activation energy model. Bioresour. Technol. 2015; 178, 126-131.

[4] Kissinger H.E. Variation of peak temperature with heating rate in differential thermal analysis. J. Res. Natl. Bur. Stand. 1956; 57, 217-221.

[5] Kissinger H.E. Reaction kinetics in differential thermal analysis. Anal. Chem. 1957; 29, 1702-1706.

[6] Coats A.W., Redfern J.P. Kinetic parameters from thermogravimetric data. Nature. 1964; 201, 68-69.

[7] Anca-Couce A., Berger A., Zobel N. How to determine consistent biomass pyrolysis kinetics in a parallel reaction scheme. Fuel. 2014; 123, 230-240.

[8] Li Z., Zhao W., Meng B., Liu C., Zhu Q., Zhao G. Kinetic study of corn straw pyrolysis: comparison of two different three-pseudo component models. Bioresource Technol. 2008; 99, 7616-7622.

[9] Lin T., Goos E., Riedel U. A sectional approach for biomass: Modelling the pyrolysis of cellulose. Fuel Process. Technol. 2013; 115, 246-253.

[10] Vand V. A theory of the irreversible electrical resistance changes of metallic films evaporated in vacuum. Proc. Phys. Soc. 1943; 55, 222-246.

[11] Vyazovkin S.V., Lesnicovich A.I. Practical application of isoconversional methods. Thermochim. Acta. 1992; 203, 177-185.

[12] Wang S., Dai G., Yang H., Luo Z. Lignocellulosic biomass pyrolysis mechanism: A state-of-the-art review. Prog. Energy Combust. Sci. 2017; 62, 33-86.

[13] Friedman H. L. Kinetics of Thermal degradation of char-foaming plastics from thermogravimetry - Application to a phenolic resin. J. Polym. Sci. 1963; 6C, 183-195.

[14] Ozawa T. A new method of analyzing thermogravimetric data. Bull. Chem. Soc. Jpn. 1965; 38, 1881-1886.

[15] Flynn J. H., Wall L. A. General treatment of the thermogravimetry of polymers. J. Res. Nat. Bur. Standards. 1966; 70A, 487-523.

[16] Akahira T., Sunose T. Method of determining activation deterioration constant of electrical insulating materials. Res. Rep. Chiba Inst. Technol. 1971; 16, 22-31.

[17] Vyazovkin S., Dollimore D. Linear and nonlinear procedures in isoconversional computations of the activation energy of nonisothermal reactions in solids. J. Chem. Inf. Comput. Sci. 1996; 36, 42-45.

[18] Vyazovkin S. Evaluation of activation energy of thermally stimulated solid-state reactions under arbitrary variation of temperature. J. Comput. Chem. 1997; 18, 393-402.

[19] Bach Q.V., Chen W.H. Pyrolysis characteristics and kinetics of microalgae via thermogravimetric analysis (TGA): A state-of-the-art review. Bioresour. Technol. 2017; 246, 88-100.

[20] Di Blasi C. Modelling chemical and physical processes of wood and biomass pyrolysis. Prog. Energy Combust. Sci. 2008; 34(1), 47-90.

[21] Bach Q.V., Chen W.H. A comprehensive study on pyrolysis kinetics of microalgae biomass. Energ. Convers. Manage. 2017; 131, 109-116.

[22] Bui H.H., Tran K.Q., Chen W.H. Pyrolysis of microalgae residues – a kinetic study. Bioresource Technol. 2016; 199, 362-366.

[23] Gai C., Zhang Y., Chen W.T., Zhang P., Dong Y. Thermogravimetric and kinetic analysis of thermal decomposition characteristics of low-lipid microalgae. Bioresour. Technol. 2013; 150, 139-148.

[24] Sharara M.A., Holeman N., Sadaka S.S., Costello T.A. Pyrolysis kinetics of algal consortia grown using swine manure wastewater. Bioresour. Technol. 2014; 169, 658-666.

[25] Liang Y.G., Cheng B., Si Y.B., Cao D.J, Jiang H.Y., Han G.M., Liu X.H. Thermal decomposition kinetics and characteristics of Spartina alterniflora via thermogravimetric analysis. Renew. Energ. 2014; 68, 111-117.

[26] Das P., Mondal D., Maiti S. Thermochemical conversion pathways of Kappaphycus alvarezii granules through study of kinetic models. Bioresour. Technol. 2017; 234, 233-242.

[27] Kassim M.A., Kirtania K, de la Cruz D., Cura N., Srivatsa S.C., Bhattacharya S. Thermogravimetric analysis and kinetic characterization of lipid-extracted Tetraselmis suecica and Chlorella sp. Algal Res. 2014; 6, 39-45.

[28] Chen C., Ma X., He Y. Co-pyrolysis characteristics of microalgae Chlorella vulgaris and coal through TGA. Bioresour. Technol. 2012; 117, 264-273.

[29] Agrawal A., Chakraborty S. A kinetic study of pyrolysis and combustion of microalgae Chlorella vulgaris using thermo-gravimetric analysis. Bioresour. Technol. 2013; 128, 72-80.

[30] Peng X., Ma X., Lin Y., Guo Z., Hu S., Ning X., Cao Y., Zhang Y. Co-pyrolysis between microalgae and textile dyeing sludge by TG–FTIR: Kinetics and products. Energ. Convers. Manage. 2015; 100, 391-402.

[31] Azazi K., Moraveji M.K., Najafabadi H.A. Characteristics and kinetics study of simultaneous pyrolysis of microalgae Chlorella vulgaris, wood and polypropylene through TGA. Bioresour. Technol. 2017; 243, 481-491.

[32] Yuan T, Tahmasebi A, Yu J. Comparative study on pyrolysis of lignocellulosic and algal biomass using a thermogravimetric and a fixed-bed reactor. Bioresource Technol. 2015; 175, 333-341.

[33] Shuping Z., Yulong W., Mingde Y., Chun L., Junmao T. Pyrolysis characteristics and kinetics of the marine microalgae Dunaliella tertiolecta using thermogravimetric analyzer. Bioresour. Technol., 2010; 101(1), 359-365.

[34] Kirtania K., Bhattacharya S. Application of the distributed activation energy model to the kinetic study of pyrolysis of the fresh water algae Chlorococcum humicola. Bioresour. Technol. 2012; 107, 476-481.

[35] Hu M., Chen Z., Guo D., Liu C., Xiao B., Hu Z., Liu S. Thermogravimetric study on pyrolysis kinetics of Chlorella pyrenoidosa and bloom-forming cyanobacteria. Bioresour. Technol. 2015; 177, 41-50.

[36] Yang X, Zhang R, Fu J, Geng S, Cheng JJ, Sun Y. Pyrolysis kinetic and product analysis of different microalgal biomass by distributed activation energy model and pyrolysis-gas chromatography-mass spectrometry. Bioresour. Technol. 2014; 163, 335-342.

[37] Soria-Verdugo A, Goos E, García-Hernando N., Riedel U. Pyrolysis of biofuels of the future: Sewage sludge and microalgae – Thermogravimetric analysis and modelling of the pyrolysis under different temperature conditions. Energ. Convers. Manage. 2017; 138, 261-272.

[38] Söyler N., Goldfarb J.L., Ceylan S., Saçan M.T. Renewable fuels from pyrolysis of Dunaliella tertiolecta: An alternative approach to biochemical conversions of microalgae. Energy. 2017; 120, 907-914.

[39] Anca-Couce A. Reaction mechanisms and multi-scale modelling of lignocellulosic biomass pyrolysis. Prog. Energy Combust. Sci. 2016; 53, 41-79.

[40] Guldberg C.M., Waage P. Ueber die chemische Affinität (About chemical affinity). J. Prakt. Chem. 1879; 19, 69-114.

[41] Flynn J.H. The temperature integral - Its use and abuse. Thermochim. Acta. 1997; 300, 83-90.

[42] Arrhenius S. Über die Reaktionsgeschwindigkeit bei der Inversion von Rohrzucker durch Säuren (On the reaction velocity of the inversion cane sugar by acids). Z. Phys. Chem. 1889; 4, 226-248.

[43] Vyazovkin S., Burnham A.K., Criado J.M., Perez-Maqueda L.A., Popescu C., Sbirrazzuoli N. ICTAC kinetics committee recommendations for performing kinetic computations on thermal analysis data. Thermochim. Acta. 2011; 520, 1-19.

[44] Doyle C.D. Estimating isothermal life from thermogravimetric data. J. Appl. Polym. Sci. 1962; 6, 639-642.

[45] Senum G.I., Yang R.T. Rational approximation of the integral of the Arrhenius function. J. Therm. Anal. 1977; 11, 445-447.

[46] Miura K. A new and simple method to estimate f(E) and k_0(E) in the distributed activation energy model from three sets of experimental data. Energ. Fuel. 1995; 9, 302-307.

[47] Miura K., Maki T. A simple method for estimating f(E) and k_0(E) in the distributed activation energy model. Energ. Fuel. 1998; 12, 864-869.

[48] Soria-Verdugo A, Goos E, Arrieta-Sanagustín J, García-Hernando N. Modeling of the pyrolysis of biomass under parabolic and exponential temperature increases using the Distributed Activation Energy Model. Energ. Convers. Manage. 2016; 118, 223-230.

[49] Beyerinck M.W. Culturversuche mit Zoochlorellen, Lichenengonidien und anderen niederen Algen. Botanische Zeitung. 1890; 45, 725-739.

[50] Hodac L., Hallmann C., Spitzer K., Elster J., Faßhauer F., Brinkmann N., Lepka D., Diwan V., Friedl T. Widespread green algae Chlorella and Stichococcus exhibit polar-temperate and tropical-temperate biogeography. FEMS Microbiol. Ecol. 2016; 92(8), 1-36.

[51] Gouveia L., Oliveira A.C. Microalgae as a raw material for biofuels production. J. Ind. Microbiol. Biotechnol. 2009; 36(2), 269-274.

[52] Parke M. Studies on marine flagellates. J. Mar. Biol. Ass. U.K. 1949; 28, 255-286.

[53] Medina A.R., Giménez Giménez A., García Camacho F., Sánchez Pérez J.A., Molina Grima E., Contreras Gómez A. Concentration and Purification of Stearidonic, Eicosapentaenoic, and Docosahexaenoic Acids from Cod Liver Oil

and the Marine Microalga Isochrysis galbana, J. Am. Oil Chem. Soc. 1995; 72, 575-583.

[54] Lubián L.M. Nannochloropsis gaditana sp. nov., una nueva Eustigmatophyceae marina. Lazaroa. 1982; 4, 287-293.

[55] Andersen R.A., Brett R.W., Potter D., Sexton J.P. Phylogeny of the Eustigmatophyceae Based upon 18S rDNA, with Emphasis on Nannochloropsis. Protist. 1998; 149, 61-74.

[56] Krienitz L., Hepperle D., Stich H.B., Weiler W. Nannochloropsis limnetica (Eustigmatophyceae) a new species of picoplankton from freshwater. Phycologia. 2000; 39, 219-227.

[57] Fietz S., Bleiß W., Hepperle D., Koppitz H., Krienitz L., Nicklisch A. First record of Nannochloropsis limnetica (Eustigmatophyceae) in the autotrophic picoplankton from Lake Baikal. J. Phycol. 2005; 41, 780-790.

[58] Fawley K.P., Fawley M.W. Observations on the Diversity and Ecology of Freshwater Nannochloropsis (Eustigmatophyceae) with Descriptions of New Taxa. Protist. 2007; 158, 325-336.

[59] European Standard EN 14214. Automotive fuels - fatty acid methyl esters (FAME) for diesel engines - requirements and test methods. 2004.

[60] European Standard EN 14111. Fat and oil derivatives - fatty acid methyl esters (FAME) - determination of iodine value. 2003.

[61] Allen E.J., Nelson E.W. On the artificial culture of marine plankton organisms. Journal of the Marine Biological Association of the U.K. 1910; 8, 421-474.

[62] Lang I., Hodac L., Friedl T., Feussner I. Fatty acid profiles and their distribution patterns in microalgae: a comprehensive analysis of more than 2000 strains from the SAG culture collection. BMC Plant Biol. 2011; 11:124, 1-16.

[63] Tomaselli L. Morphology, Ultrastructure and Taxonomy of Arthrospira (Spirulina) maxima and Arthrospira (Spirulina) platensis, 1-15. In: Spirulina Platensis (Arthrospira): Physiology, Cell-Biology and Biotechnology, Ed. Vonshak A., Taylor Francis, 1997.

[64] Geitler L. Cyanophyceae von Europa unter Berücksichtigung der anderen Kontinete. (Cyanophyceae from Europe under consideration of the other continents), 1-1196. In: Die Algen (the algae), Ed. Kolkwitz R., Dr. L. Rabenhorst´s Kryptogamen-Flora von Deutschland, Österreich und der Schweiz (cryptogam-flora of Germany, Austria and Switzerland), 2nd edition, Akad. Verlagsgesellschaft. 1932.

[65] Nelissen B., Wilmotte A., Neefs J.M., de Wachter R., Phylogenetic relationships among filamentous helical cyanobacteria investigated on the basis of 16S ribosomal RNA gene sequence analysis. Systematic and Applied Microbiology. 1994; 17, 206-211.

[66] Ciferri O. Spirulina, the Edible Microorganism. Microbiological Reviews. 1983; 47(4), 551-578.

[67] Gershwin M.E., Belay A. Spirulina in human nutrition and health. CRC Press, USA. 2007.

[68] Scheldeman P., Baurain D., Bouhy R., Scott M., Mühling M., Whitton B.A., Belay A., Wilmotte A. Arthrospira ('Spirulina') strains from four continents are

resolved into only two clusters, based on amplified ribosomal DNA restriction analysis of the internally transcribed spacer. FEMS Microbiology Letters 1999; 172(2), 213-222.

[69] Cohen Z., Vonshak A., Richmond A. Fatty acid composition of Spirulina strains grown under various environmental conditions. Phytochemistry. 1987; 26(8), 2255-2258.

[70] Zhao B., Wang X., Yang X. Co-pyrolysis characteristics of microalgae Isochrysis and Chlorella: kinetics, biocrude yield and interaction. Bioresour. Technol. 2015; 198, 332-339.

[71] Batista A.P., Gouveia L., Bandarra N.M., Franco J.M., Raymundo A. Comparison of microalgal biomass profiles as novel functional ingredient for food products. Algal Res. 2013; 2, 164-173.

[72] Sanchez-Silva L., López-González D., Garcia-Minguillan A.M., Valverde J.L. Pyrolysis, combustion and gasification characteristics of Nannochloropsis gaditana microalgae. Bioresour. Technol. 2013; 130, 321-331.

[73] López-González D., Fernandez-Lopez M., Valverde J.L., Sanchez-Silva L. Pyrolysis of three different types of microalgae: Kinetic and evolved gas analysis. Energy. 2014; 73, 33-43.

[74] Chen W., Yang H., Chen Y., Xia M., Yang Z., Wang X., Chen H. Algae pyrolytic poly-generation: Influence of component difference and temperature on products characteristics. Energy. 2017; 131, 1-12.

[75] Bagnoud-Velásquez M., Schmid-Staiger U., Peng G., Vogel F., Ludwig Ch. First developments towards closing the nutrient cycle in a biofuel production process. Algal Res. 2015; 8, 76-82.

[76] Becker E.W. Micro-algae as a source of protein. Biotechnol. Adv. 2007; 25, 207-210.

[77] Gai C., Zhang Y., Chen W.T., Zhang P., Dong Y. Thermogravimetric and kinetic analysis of thermal decomposition characteristic of low-lipid microalgae. Bioresource Technol. 2013; 150, 139-148.

[78] Toor S.S., Reddy H., Deng S., Hoffmann J., Spangsmark D., Madsen L.B., Holm-Nielsen J.B., Rosendahl L.A. Hydrothermal liquefaction of Spirulina and Nannochloropsis salina under subcritical and supercritical water conditions. Bioresource Technol. 2013; 131, 413-419.

[79] Pistorius A.M.A., DeGrip W.J., Egorova-Zachernyuk T.A. Monitoring of biomass composition from microbiological sources by means of FT-IR spectroscopy. Biotechnol. Bioeng. 2009; 103, 123-129.

[80] Deng X.Y., Gao K., Addy M., Li D., Zhang R.C., Lu Q., Ma Y.W., Cheng Y.L., Chen P., Liu Y.H., Ruan R. Cultivation of Chlorella vulgaris on anaerobically digested swine manure with daily recycling of the post-harvest culture broth. Bioresource Technol. 2018; 247, 716-723.

[81] Deng X.Y., Gao K., Zhang R.C., Addy M., Lu Q., Ren H.Y., Chen P., Liu Y.H., Ruan R. Growing Chlorella vulgaris on thermophilic anaerobic digestion swine manure for nutrient removal and biomass production. Bioresource Technol. 2017; 243, 417-425.

[82] Bonfanti C., Cardoso C., Afonso C., Matos J., García T., Tanni S., Bandarra N.M. Potential of microalga Isochrysis galbana: Bioactivity and bioaccessibility. Algal Res. 2018; 29, 242-248.

[83] Freire I., Cortina-Burgueño A., Grille P., Arizcun M.A., Abellán E., Segura M., Sousa F.W., Otero A. Nannochloropsis limnetica: A freshwater microalga for marine aquaculture. Aquaculture 2016; 459, 124-130.

[84] Soria-Verdugo A., Goos E., Garcia-Hernando N. Effect of the number of TGA curves employed on the biomass pyrolysis kinetics results obtained using the Distributed Activation Energy Model. Fuel Process. Technol. 2015; 134, 360-371.

[85] Soria-Verdugo A., Garcia-Gutierrez L.M., Blanco-Cano L., Garcia-Gutierrez N., Ruiz-Rivas U. Evaluating the accuracy of the Distributed Activation Energy Model for biomass devolatilization curves obtained at high heating rates. Energ. Convers. Manage. 2014; 86 1045-1049.

[86] Hu S., Jess A., Xu M. Kinetic study of Chinese biomass slow pyrolysis: Comparison of different kinetic models. Fuel. 2007; 86, 2778-2788.

[87] Mani T., Murugan P., Abedi J., Mahinpey N. Pyrolysis of wheat straw in a thermogravimetric analyzer: effect of particle size and heating rate on devolatilization and estimation of global kinetics. Chem. Eng. Res. Des. 2010; 88, 952-958.

[88] Soria-Verdugo A., Garcia-Hernando N., Garcia-Gutierrez L.M., Ruiz-Rivas U. Analysis of biomass and sewage sludge devolatilization using the distributed activation energy model. Energ. Convers. Manage. 2013; 65, 239-244.

[89] Comesaña R., Gómez M.A., Álvarez M.A., Eguía P. Thermal lag analysis on a simulated TGA-DSC device. Thermochim. Acta. 2012; 547, 13-21.

[90] Munir S., Daood S.S., Nimmo W., Cunliffe A.M., Gibbs B.M. Thermal analysis and devolatilization kinetics of cotton stalk, sugar cane bagasse and shea meal under nitrogen and air atmosphere. Bioresour. Technol. 2009; 100, 1413-1418.

[91] Tonbul Y., Saydut A., Yurdako K., Hamamci C. A kinetic investigation on the pyrolysis of Seguruk asphaltite. J. Therm. Anal. Calorim. 2009; 95, 197-202.

[92] Ferreira A.F., Soares Dias A.P., Silva C.M., Costa M. Evaluation of thermochemical properties of raw and extracted microalgae. Energy. 2015; 92 365-372.

[93] Figueira C.A., Moreira P.F., Giudici R. Thermogravimetric analysis of the gasification of microalgae Chlorella Vulgaris. Bioresource Technol. 2015; 198, 717-724.

[94] Maurya R., Ghosh T., Saravaia H., Paliwal C., Ghosh A., Mishra S. Non-isothermal pyrolysis of de-oiled microalgal biomass kinetics and evolved gas analysis. Bioresour. Technol. 2016; 221, 251-61.